

Recent Changes in Mean and Extreme Temperature and Precipitation in the Western Pacific Islands

SIMON MCGREE,^{a,b} NICHOLAS HEROLD,^c LISA ALEXANDER,^c SERGEI SCHREIDER,^a YURIY KULESHOV,^{a,d,e,f} ELIFALETI ENE,^g SELU FINAULAHI,^h KASIS INAPE,ⁱ BOYD MACKENZIE,^j HANS MALALA,^k ARONA NGARI,^l BIPENDRA PRAKASH,^m AND LLOYD TAHANIⁿ

^a Department of Mathematical Sciences, School of Science, RMIT University, Melbourne, Victoria, Australia

^b Climate and Oceans Support Program in the Pacific, Bureau of Meteorology, Melbourne, Victoria, Australia

^c Climate Change Research Centre and Australian Research Council Centre of Excellence for Climate Extremes, University of New South Wales, Sydney, New South Wales, Australia

^d School of Mathematics and Statistics, University of Melbourne, Parkville, Victoria, Australia

^e Faculty of Sciences, Engineering and Technology, Swinburne University of Technology, Melbourne, Victoria, Australia

^f Climate Information Services, Bureau of Meteorology, Melbourne, Victoria, Australia

^g Tuvalu Meteorological Service, Funafuti, Tuvalu

^h Tonga Meteorological Service, Fua'amotu Airport, Fua'amotu, Tonga

ⁱ National Weather Service, Port Moresby, Papua New Guinea

^j NOAA Weather Service Office, Weno, Chuuk, Federated States of Micronesia

^k NOAA Weather Service Office, Pagopago, American Samoa

^l Cook Islands Meteorological Service, Rarotonga, Cook Islands

^m Fiji Meteorological Service, Nadi Airport, Nadi, Fiji

ⁿ Solomon Islands Meteorological Service, Honiara, Solomon Islands

(Manuscript received 2 November 2018, in final form 1 May 2019)

ABSTRACT

Trends in mean and extreme annual and seasonal temperature and precipitation over the 1951–2015 period were calculated for 57 stations in 20 western Pacific Ocean island countries and territories. The extremes indices are those of the World Meteorological Organization Expert Team on Sector-Specific Climate Indices. The purpose of the expert team and indices is to promote the use of globally consistent climate indices to highlight variability and trends in climate extremes that are of particular interest to socioeconomic sectors and to help to characterize the climate sensitivity of various sectors. Prior to the calculation of the monthly means and indices, the data underwent quality control and homogeneity assessment. A rise in mean temperature occurred at most stations, in all seasons, and in both halves of the study period. The temperature indices also showed strong warming, which for the majority was strongest in December–February and weakest in June–August. The absolute and percentile-based indices show the greatest warming at the upper end of the distribution. While changes in precipitation were less consistent and trends were generally weak at most locations, declines in both total and extreme precipitation were found in southwestern French Polynesia and the southern subtropics. There was a decrease in moderate- to high-intensity precipitation events, especially those experienced over multiple days, in southwestern French Polynesia from December to February. Strong drying trends have also been identified in the low- to moderate-extreme indices in the June–August and September–November periods. These negative trends contributed to an increase in the magnitude of meteorological drought in both subregions.

 Denotes content that is immediately available upon publication as open access.

Corresponding author: Simon McGree, simon.mcgree@bom.gov.au

1. Introduction

The character and severity of impacts from climate extremes depend not only on the extremes themselves but also on society's exposure and vulnerability (Field et al. 2012). While small island developing states vary in

their geography, climate, culture, and stage of economic development, they have many common characteristics that highlight their exposure and vulnerability, particularly as it relates to sustainable development and climatic change. These characteristics include limited physical size, generally limited natural resources, high susceptibility to natural hazards, relatively thin water lenses, extreme openness of small economies, high sensitivity to external market shocks, and in some cases high population densities, high population growth rates, and frequently poorly developed infrastructure (IPCC 2001). Therefore, it is imperative that a sound understanding of past, recent, and likely future changes in the western Pacific Ocean climate is attained so as to inform decision-making and to stand the best chance of sustaining life on these islands in the coming century and beyond.

Trends in western Pacific observed total precipitation and mean temperature have been studied on several occasions in the past (e.g., Salinger et al. 1995; Folland et al. 2003; Australian Bureau of Meteorology and CSIRO 2011a,b; Lough et al. 2011; Jones et al. 2013). The first attempt at examining changes in precipitation and temperature extremes was through a series of five workshops, from 1998 to 2004, funded by the Asia-Pacific Network (APN) for Global Change Research (Manton et al. 2001; Page et al. 2004; Griffiths et al. 2003, 2005). The initial workshop led to a series of climate change workshops across the globe under the guidance of the former World Meteorological Organization (WMO) Commission for Climatology (CCI), World Climate Research Programme, and the WMO/Intergovernmental Oceanographic Commission Joint Technical Commission for Oceanography and Marine Meteorology Expert Team on Climate Change Detection and Indices (ETCCDI) (Peterson and Manton 2008; Zhang et al. 2011). The ETCCDI, which was formed in 1999, developed a set of core indices consisting of 27 descriptive indices aimed at detecting changes in “moderate extremes.” These internationally agreed standard definitions and procedures allow results to be compared consistently across different regions and countries (Peterson and Manton 2008; Zhang et al. 2011; Alexander 2016). In the western Pacific, the ETCCDI indices were used at a WMO World Climate Data and Monitoring Programme workshop in Hanoi, Vietnam, in December 2007 (Caesar et al. 2011) and at an APN workshop in Seoul, South Korea, in February 2008 (Choi et al. 2009). These workshops were largely focused on Asia–Australia, with minimal inclusion of the Pacific islands (Fiji at the Hanoi workshop, and Australia and New Zealand subtropical Pacific islands at the Seoul workshop). The most recent work on changes in Pacific

islands temperature and precipitation extremes (Australian Bureau of Meteorology and CSIRO 2014; McGree et al. 2014; Whan et al. 2014a) was conducted through the Australian Aid funded Pacific–Australia Climate Change Science and Adaptation Planning (PACCSAP) Program; it also used the ETCCDI methodology and recommended software. The Pacific Climate Change Data Portal <http://www.bom.gov.au/climate/pccsp/>, which presents trends in the mean and extreme temperature and precipitation for the western Pacific islands, is an outcome of the PACCSAP Program.

While some of the ETCCDI indices are potentially useful for sector applications (e.g., number of days with frost for agricultural applications or heat waves for health applications), many of the others have no obvious sector relevance. As a result, the WMO CCI set up the Expert Team on Sector-Specific Climate Indices (ET-SCI, <http://www.wmo.int/pages/prog/wcp/ccl/opace/opace4/ET-SCI-4-1.php>). In cooperation with sectoral experts in agricultural meteorology, water resources, and health, the ET-SCI is working to identify and evaluate additional sector-specific indices, both single- and multivariable types, to define both simple and complex climate risks of interest to user groups. Relying on the principles of ETCCDI, this work focuses on systematic and globally consistent approaches using high-quality data and appropriate statistical methods to help characterize the susceptibility of various sectors to climate variability and change in an authoritative manner (Alexander 2016). The first proof of concept ET-SCI workshop for six South American countries was held in Ecuador in June 2013.

As part of the Programme of Implementing the Global Framework on Climate Services on Regional and National Scales funded by Environment Canada, the ET-SCI organized a second workshop on Enhancing Climate Indices for Sector-Specific Applications in the Pacific island region, in Nadi, Fiji, from 7 to 11 December 2015. This paper presents results from and further analyses associated with this workshop. Much like the earlier APN and PACCSAP Program workshops, the ET-SCI Pacific workshop’s objectives were to build and develop capacity in the quality control and homogenization of climate data, calculate core ET-SCI indices using standardized software (ClimPACT2), and conduct the first stage of analysis of sectoral data. The workshop brought together experts from national meteorological and hydrological services of American Samoa, Cook Islands, Federated States of Micronesia, Fiji, Papua New Guinea, Samoa, Solomon Islands, Tonga, Tuvalu, and Vanuatu, along with national representatives from agriculture and food security, water and health. The WMO, University of New South Wales (Sydney,

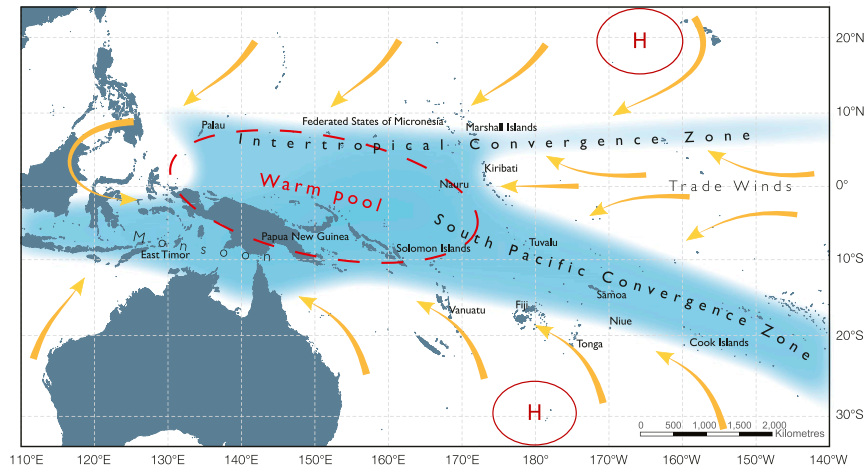


FIG. 1. Schematic of circulation in the Pacific (from Australian Bureau of Meteorology and CSIRO (2011a,b).

Australia), Australian Bureau of Meteorology, New Zealand Institute for Water and Atmosphere, Pacific Regional Environmental Programme (SPREP), and Caribbean Institute for Meteorology and Hydrology were also represented.

A recent study (McGree et al. 2014) on changes in western Pacific total precipitation (1961–2011) found station-scale trends were largely nonsignificant (for >95% of stations) and lacked spatial coherence north of the southern subtropics. On a subregional level, a negative trend in the southern subtropics was statistically significant over 1951–2011. This was in contrast to results from the APN workshops a decade earlier (Manton et al. 2001; Griffiths et al. 2003) that found precipitation trends over 1961–98 and 1961–2000, respectively to be spatially consistent east of the date line, with a break across the South Pacific convergence zone (SPCZ; Fig. 1). Trends in total precipitation were largely positive to the north of the eastern diagonal portion of the SPCZ and negative to the southwest of the diagonal portion. West of the date line, a region influenced by the western zonal portion of the SPCZ, trends were typically less coherent and not significant. The trends at that time were associated with northeast movement of the diagonal SPCZ since the late 1970s through to the 1990s, associated with a shift to a positive interdecadal Pacific oscillation (IPO) phase (Folland et al. 2002; Salinger et al. 2014; Henley et al. 2015).

The primary reason that the McGree et al. (2014) results were different was the switch to a negative IPO phase from 1999, a period dominated by La Niña events (Salinger et al. 2014). This was reflected in trends over 1981–2011 that showed it had become wetter in the west Pacific monsoon (WPM; Fig. 1) region and southwest

of the SPCZ. In the tropical North Pacific, it has also become wetter west of 160°E, with the intertropical convergence zone (ITCZ; Fig. 1)/WPM expanding northward west of 140°E. Northeast of the SPCZ and in the central tropical Pacific east of about 160°E, trends were negative. This points to risks in overinterpreting short-term trends in regions with significant influence from modes of variability on interannual-to-multidecadal time scales.

Trends in the extreme precipitation showed little spatial consistency with few statistically significant trends. On a subregional scale, only the simple daily precipitation intensity (SDII) index (positive trend) in the WPM and number of wet days (R1mm) and number of days on which precipitation was greater or equal to 10 mm (R10mm) (negative trends) in the South Pacific subtropics showed statistically significant trends over 1951–2011 (McGree et al. 2014). Previous studies found a strong relationship between El Niño–Southern Oscillation (ENSO) and total precipitation and between ENSO and the threshold ETCCDI indices (Griffiths et al. 2003; McGree et al. 2014). The percentile-based and absolute ETCCDI indices are also influenced by ENSO but to a lesser extent than total precipitation (McGree et al. 2014). It can be said that, generally in the western Pacific tropics, wetter years receive rain on more days, with higher extreme precipitation intensities and more frequent extreme events. More extreme total precipitation is also significantly correlated to more extreme extended-duration precipitation events (Griffiths et al. 2003).

Previous studies have found mean air temperature trends were spatially homogenous across the region with mean warming of $0.18^{\circ}\text{C} (10\text{yr})^{-1}$ over 1961–2011 (Whan et al.

2014a). This trend is consistent with the $0.16^{\circ}\text{C} (10\text{yr})^{-1}$ from Jones et al. (2013), albeit for a slightly different set of stations for 1961–2010. Spatially coherent warming trends in the maximum and minimum air temperature extremes were also found over 1951–2011 on a regional and subregional level (Whan et al. 2014a). Where comparison is possible, these works were largely consistent with results from early studies (Manton et al. 2001; Griffiths et al. 2005).

Larger warming trends were generally found in the hottest day and hottest night of the year compared with the coolest day and coolest night of the year. Warming trends were also found for all the percentile indices, although there were fewer differences between the number of days and nights per year where maximum or minimum exceeded percentile thresholds (Whan et al. 2014a).

Significant relationships between ENSO and indices of extreme temperature have been found in the East Asia–western Pacific region (Nicholls et al. 2005; Whan et al. 2014a). Nicholls et al. (2005) found an increase in the number of warm nights and hot days during an El Niño event, with the number of cool days and nights tending to decrease. The Whan et al. (2014a) study also highlighted the role of decadal variability in the trends of the percentile indices: steady increases in the value of extreme temperatures are combined with considerable variability in the number of days per year that exceed extreme temperature thresholds. This showed the complex nature of temperature extremes in a region with low temperature variability.

None of these studies, however, present results that are explicitly sector relevant. They examined trends on a subregional scale from 1951 and did not examine trends on a seasonal scale. The objectives of this study, therefore, are to examine trends in the mean and extremes for the ET-SCI sector-relevant indices from 1951 to 2015, using quality-controlled and homogenized daily temperature and precipitation data from the western Pacific.

The study region covers the Pacific from about 134°E to 135°W and from 15°N to 32°S , excluding Indonesia and the Australian mainland. The paper is organized as follows: section 2 provides a description of the data used and outlines the research methods, section 3 examines the linear trends in the indices, and the discussion of the results and conclusions are presented in section 4.

2. Data and method

a. Data

Station data were collated from multiple sources. Data from 1951 to about 2013 were obtained from the Pacific

Climate Change Data Portal (<http://www.bom.gov.au/climate/pccsp/>), which has previously been used by Jones et al. (2013), McGree et al. (2014), and Whan et al. (2014b). Prior to the ET-SCI workshop, participants representing 10 countries were asked to update their data to 2015. Data for 11 additional countries and territories (French Polynesia, Guam, Kiribati, Marshall Islands, Nauru, New Caledonia, Niue, Northern Mariana Islands, Palau, Pitcairn Islands, and Wallis and Futuna) not represented at the workshop were obtained from the respective national agencies following the workshop. Only station records from 1951 to 2015 that were at least 80% complete were retained to ensure a robust analysis of Pacific trends was undertaken. All the data obtained was archived in the Pacific Climate Change Data Portal.

To determine whether there is a relationship between IPO and mean and extreme temperature and precipitation, the tripole index (TPI; NOAA ERSST version 5, unfiltered) (Henley et al. 2015) for the period 1951–2015 was obtained from <https://www.esrl.noaa.gov/psd/data/timeseries/IPOTPI/>.

b. Data quality and homogeneity

Before undertaking any analyses of extremes, whether at a regional or global level, it is important to ensure that the input data are of high quality and free from artificial inconsistencies (Alexander 2016).

Basic quality control of all the data was undertaken at the data source. Further quality control was performed at and following the Nadi workshop using the freely available RCLimDex, version 1.1 (v1.1), software package (Zhang and Yang 2004), and the “extraQC” version of RCLimDex (Aguilar and Prohom 2011). The latter performs an additional series of tests to further ensure internal consistency (e.g., identifies consecutive identical values and rounded values) and temporal coherency (locates large interdaily differences), in addition to the usual gross-error and tolerance tests.

Errors in station records such as negative daily precipitation values and daily minimum temperature values greater than daily maximum temperature were identified using RCLimDex. Outliers in precipitation and maximum and minimum temperature based on user-defined thresholds were also identified. A daily precipitation upper threshold of 200 mm was defined; however, because tropical disturbances are common in the tropical Pacific and not all of these events documented, it is near impossible to identify suspicious values during the tropical cyclone/typhoon season. Confirmation that precipitation events ≥ 200 mm were related to real meteorological events, rather than being erroneous, was undertaken where possible.

For maximum and minimum temperature, a threshold of 5 standard deviations was defined. On occasion, it was

apparent the maximum temperature value was the correct minimum temperature value or vice versa; a data-entry error had occurred, for example, swapping the two digits before the decimal point, or the decimal point was misplaced or not added (also applied to precipitation). In such cases, the erroneous value was replaced with a realistic value and where possible confirmation with the original observation field book was undertaken. Outliers identified as very likely erroneous were removed. Overall, fewer than 1% of the daily temperature and daily precipitation records were corrected for errors and outliers.

To reliably determine long-term change in climate it is important to have data whose changes reflect changes in the climate and not changes due to circumstances under which the observations were taken. There are numerous factors that can affect observation records. Among the most common are changes in instrumentation, changes in the surrounding environment, site relocations, and changes in observing practices (Trewin 2010; Vincent et al. 2012). To homogenize a station record, detailed metadata of the station in question is required, ideally along with the complete records of the station and its closest neighbors. Homogenization of Pacific islands meteorological data is difficult as most stations are isolated and often belong to different climate regimes from their neighbors. In addition, metadata are often sparse or nonexistent (Jones et al. 2013).

While removing inhomogeneous stations has generally been the approach taken by the ETCCDI at most of their regional workshops (Peterson and Manton 2008), this practice would severely restrict the number of western Pacific temperature records available for analyses. Clearly data homogenization is acceptable, because many regions—for example, the Caribbean (Stephenson et al. 2014)—and countries—for example, Australia (Trewin 2013)—have adjusted daily and/or monthly time series in their high-quality datasets.

As for McGree et al. (2014) and Whan et al. (2014a), each series was assessed for potential inhomogeneities using subjective and objective tests. This involved a combination of visual examinations, neighbor comparisons, and the application of the RHtestsV4 software package (Wang and Feng 2013). Step changes were identified using monthly time series (precipitation was log transformed), so as to avoid the challenge of additional noise present in the daily series. In addition, data were at times more complete at monthly than at daily time scales. Using the change points detected in the monthly time series, the daily time series were adjusted as required.

Step changes were detected using multiple tests to increase confidence in the adjustments. The first test

involved using the RHtestsV4 penalized maximal F test (Wang 2008a,b) to locate step changes in the record that were significant at the 99% confidence level. The second test involved using the RHtestsV4 penalized maximal t test (Wang et al. 2007; Wang 2008a) where the closest neighboring homogenous station was used as a reference series, where available, to identify step changes in the base series. The third test was based upon the strong relationship between island coastal temperatures and local sea surface temperatures (SSTs) (Kenyon and Hegerl 2008; Alexander et al. 2009; Jones et al. 2013; Whan et al. 2014a). SSTs (1951–2015) from the HadISST1 1° reconstruction dataset (Rayner et al. 2003) were used to create a local time series ($10^\circ \times 10^\circ$ area-averaged SST series centered over each station) that was tested and, if found homogeneous, used as a reference series. For the fourth test, step changes (99% confidence level) in the diurnal temperature range were assessed, as changes in measurement practice can preferentially alter either maximum or minimum temperature (Zhou and Ren 2011; Jones et al. 2013).

Even with the log transformation of precipitation, detection of precipitation inhomogeneities using the penalized maximal F test was difficult because of high variability in the data series and large distances between neighboring stations. In most cases where an inhomogeneity was detected, the discontinuity was not consistent between tests; therefore no action was taken. In most cases only the maximal F test was applied to the precipitation records because almost all of the precipitation stations were too isolated to apply the penalized maximal t test and the third and fourth tests apply only to temperature. Precipitation records were excluded from further analyses where consistent inhomogeneities were found. Excluded records include Nanumea and Niulakita from Tuvalu, La Tontouta from New Caledonia, and Pitcairn Island.

Temperature time series were adjusted where metadata or most of the detection tests provided good reason for the modification. Greatest confidence was gained from metadata. However, we note that metadata is most likely incomplete or lacking detail as record keeping tends to focus on the observation enclosure, at times omitting changes in the surrounding environment. Detected discontinuities were often inconsistent between each of the inhomogeneity tests. Without metadata support, temperature records were only adjusted if at least three of the four tests identified a discontinuity at a particular point in time. For stations with few metadata, there is a greater reliance on the statistical tests.

While reference series were used to detect discontinuities, the quantile-matching “without a reference series” method in RHtestsV4 was used to adjust (only for

TABLE 1. List of stations, their locations, and period of record (if the period of the monthly record is different from the period of the daily record it is given in parentheses).

| Country | Station | Lon | Lat | Period of daily precipitation | Period of daily temperature |
|-----------------------------------|-------------------------------------|----------|---------|-------------------------------|-----------------------------|
| American Samoa | Pagopago | 170.71°E | 14.33°S | 1956–2015 | 1957–2015 |
| Australia | Willis Island | 149.98°E | 16.30°S | 1951–2015 | 1951–2015 |
| | Norfolk Island Aero | 167.94°E | 29.04°S | 1951–2015 | 1951–2015 |
| | Lord Howe Island Aero | 159.08°E | 31.54°S | 1951–2015 | 1951–2015 |
| Cook Islands | Penrhyn | 158.05°W | 9.03°S | 1951–2015 | — |
| | Rarotonga | 159.80°W | 21.20°S | 1951–2015 | 1951–2015 |
| Federated States of Micronesia | Pohnpei | 158.22°E | 6.97°N | 1951–2015 | 1951–2015 |
| | Yap | 138.08°E | 9.48°N | 1951–2015 | (1951–2015) |
| | Chuuk | 151.83°E | 7.45°N | 1951–2015 | 1951–2015 |
| Fiji | Rotuma | 177.05°E | 12.50°S | 1951–2015 | — |
| | Penang Mill | 178.17°E | 17.37°S | 1951–2015 | — |
| | Lautoka Mill | 177.45°E | 17.60°S | 1951–2015 | 1951–2015 |
| | Nadi Airport | 177.45°E | 17.77°S | 1951–2015 | 1951–2015 |
| | Nausori Airport | 178.57°E | 18.05°S | 1956–2015 | 1957–2015 |
| | Laucala Bay, Suva | 178.45°E | 18.15°S | 1951–2015 | 1951–2015 |
| | Nabouwalu | 178.70°E | 17.00°S | 1951–2015 | 1952–2015 |
| | Lakeba | 178.80°W | 18.23°S | 1951–2015 | — |
| French Polynesia | Atuona (Hiva Oa, Marquesas Islands) | 139.03°W | 9.82°S | 1951–2015 | — |
| | Takaraoa (Tuamotu Group) | 145.03°W | 14.48°S | 1951–2015 | 1951–2015 |
| | Tahiti-Faaa (Society Islands) | 149.61°W | 17.55°S | 1957–2015 (1951–56) | 1957–2015 |
| | Mataura (Tubuai, Austral Islands) | 149.48°W | 23.35°S | 1951–2015 | — |
| | Rapa (Austral Islands) | 144.33°W | 27.62°S | 1951–2015 | 1951–2015 |
| Guam | Agana (Guam International Airport) | 144.80°E | 13.48°N | 1957–2015 | — |
| Kiribati | Butaritari | 172.78°E | 3.03°N | (1951–2015) | — |
| | Kiritimati | 157.48°W | 1.98°N | 1951–2015 | — |
| | Tarawa | 172.92°E | 1.35°N | 1951–2015 | 1951–2015 |
| Marshall Islands | Kwajalein/Bucholz Aaf | 167.73°E | 8.73°N | 1951–2015 | 1951–2015 |
| | Majuro | 171.38°E | 7.08°N | 1951–2015 | 1951–2015 |
| Nauru | Nauru Arc-2 | 166.92°E | 0.52°N | (1951–2015) | — |
| New Caledonia | Koumac | 164.28°E | 20.56°S | 1951–2015 | 1951–2015 |
| | Touho Gend | 165.23°E | 20.78°S | 1952–2015 | — |
| | La Foa | 165.81°E | 21.70°S | 1951–2015 | 1952–2015 |
| | Kone | 164.83°E | 21.05°S | 1951–2015 | — |
| | Ponerihouen | 165.40°E | 21.08°S | 1952–2015 | — |
| | Houailou P | 165.63°E | 21.28°S | 1952–2015 | — |
| | Noumea | 166.45°E | 22.28°S | 1951–2015 | 1951–2015 |
| New Zealand | Raoul Island | 177.92°W | 29.25°S | 1951–2015 | 1951–2015 |
| Niue | Hanan Airport | 169.93°W | 19.08°S | 1951–2015 | 1951–2015 |
| Northern Mariana Islands | Saipan International Airport | 145.73°E | 15.12°N | 1954–2015 | — |
| Palau | Koror | 134.48°E | 7.33°N | 1951–2015 | 1951–2015 |
| Papua New Guinea | Momote | 147.42°E | 2.05°S | 1951–2015 | — |
| | Kavieng | 150.82°E | 2.57°S | 1951–2014 | — |
| | Wewak | 143.67°E | 3.58°S | 1951–2015 | — |
| | Madang | 145.80°E | 5.22°S | 1951–2015 | — |
| | Port Moresby | 147.22°E | 9.38°S | 1951–2015 | 1951–2015 |
| | Misima | 152.83°E | 10.68°S | 1951–2015 | — |
| Solomon Islands | Honiara | 159.97°E | 9.42°S | 1951–2015 | — |
| | Honiara_Henderson | 160.05°E | 9.42°S | — | 1951–2015 |
| Tonga | Keppel | 173.77°W | 15.95°S | 1951–2015 | — |
| | Lupepau'u (Vava'u) | 173.97°W | 18.58°S | 1951–2015 | 1956–2015 |
| | Haapai | 174.35°W | 19.80°S | 1951–2015 | — |
| | Nuku'alofa | 175.18°W | 21.13°S | (1951–2015) | (1951–2015) |
| Tuvalu | Funafuti | 179.22°E | 8.50°S | 1951–2015 | 1951–2015 |
| Vanuatu | Sola | 167.55°E | 13.85°S | 1951–2015 | — |
| | Port Vila_Bauerfield | 168.30°E | 17.70°S | — | 1951–2015 |
| | Port Vila | 168.32°E | 17.74°S | 1951–2015 | — |
| | Aneityum | 169.77°E | 20.23°S | 1951–2015 | — |

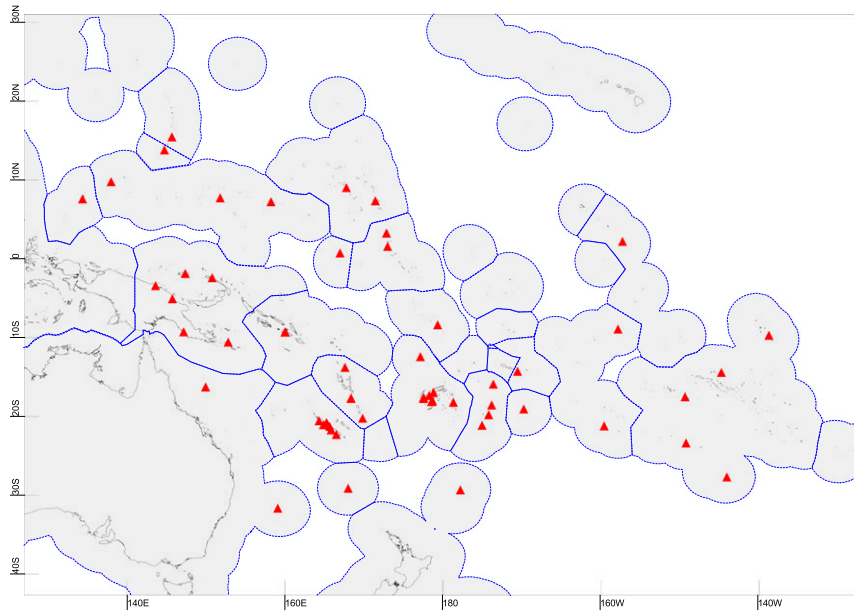


FIG. 2. Locations of the 57 stations. Station names and locations are presented in Table 1.

discontinuities identified by three of the four tests) both the daily and monthly temperature time series. The sparse data network inhibited the use of reference series for the adjustment. As for Whan et al. (2014a), when it came to adjustments, SSTs have not been used as reference series so as not to bias the air temperature records with those of the sea surface.

Fifty-five monthly precipitation, 31 monthly temperature, 52 daily precipitation, and 29 daily temperature stations were available for analysis with >80% of data available over the 1951–2015 period (Table 1; Fig. 2). While it is possible that several inhomogeneities have escaped detection, these data are believed to be largely homogeneous.

c. Calculation of ET-SCI indices

The ET-SCI indices were then calculated by applying ClimPACTv2 to the homogenized series (Alexander and Herold 2015). ClimPACTv2 facilitates the calculation of over 60 ET-SCI sector-specific (including the ETCCDI) indices. The “core set” is made up of 34 indices (including four user-defined indices), while the remaining 30 are defined as “additional indices.” These include five heat-wave indices, three additional extreme temperature indices and 14 ETCCDI indices. The full list of ET-SCI indices is presented in Table 2.

There are several user-defined indices: For WSDId and CSDId, a period of 3 days has been selected; for Rnmm, 1 mm has been selected; and for RXdday, 2 days was used.

The annual and seasonal trends in total precipitation and mean, maximum, and minimum temperature were

calculated from monthly values rather than the corresponding indices, as there are fewer gaps in the monthly records.

Monthly indices were calculated if no more than 3 days were missing in a month, while annual values were calculated if no more than 15 days were missing in a year. In the case of monthly totals and averages only, annual values were not calculated if one or more months of data were missing. For threshold indices, a threshold was calculated if at least 75% of the data was present. For spell duration indicators, a spell can continue into the next year and was counted against the year in which the spell ended. Percentiles were calculated if no more than 20% of the values were missing over 1971–2000.

d. Trend calculations and regional series

Linear annual and seasonal trends were calculated using the nonparametric Kendall’s tau-based slope estimator (Sen 1968). This method has notable advantages over the more commonly used least squares estimate. It is nonparametric and is less affected by outliers, making it well suited to meteorological and hydrological time series. The significance of the trend is determined using Kendall’s test. This test does not assume an underlying probability distribution of the data series. Calculations were performed using an “autotrend” R script developed by Environment Canada (Zhang et al. 2000). Autotrend also accounts for autocorrelation also known as serial correlation. This is defined as the correlation of a variable with itself over successive time intervals. Autocorrelation increases the chances of finding

TABLE 2. Core and additional ET-SCI indices. Index codes in boldface refer to those that are solely ET-SCI indices (and not also ETCCDI indices). Here, TM = mean temperature, TN = minimum temperature, TX = maximum temperature, and PR = precipitation. Indices in italics have not been used in this study.

| Index codes | Indicator name | Definition | Units |
|------------------------|---|--|--------------------|
| Core indices | | | |
| <i>FD</i> | Frost days | No. of days on which $TN < 0^{\circ}\text{C}$ | Days |
| <i>TNlt2</i> | TN below 2°C | No. of days on which $TN < 2^{\circ}\text{C}$ | Days |
| <i>TNltm2</i> | TN below -2°C | No. of days on which $TN < -2^{\circ}\text{C}$ | Days |
| <i>TNltm20</i> | TN below -20°C | No. of days on which $TN < -20^{\circ}\text{C}$ | Days |
| <i>ID</i> | Ice days | No. of days on which $TX < 0^{\circ}\text{C}$ | Days |
| SU | Summer days | No. of days on which $TX > 25^{\circ}\text{C}$ | Days |
| TR | Tropical nights | No. of days on which $TN > 20^{\circ}\text{C}$ | Days |
| <i>GSL</i> | Growing-season length | Annual no. of days between the first occurrence of 6 consecutive days with $TM > 5^{\circ}\text{C}$ and the first occurrence of 6 consecutive days with $TM < 5^{\circ}\text{C}$ | Days |
| TXx | Max TX | Warmest daily TX | $^{\circ}\text{C}$ |
| TNn | Min TN | Coldest daily TN | $^{\circ}\text{C}$ |
| <i>WSDI</i> | Warm-spell duration indicator | Annual no. of days contributing to events in which 6 or more consecutive days experience $TX > 90\text{th percentile}$ | Days |
| <i>WSDId</i> | User-defined WSDI | Annual no. of days contributing to events in which d or more consecutive days experience $TX > 90\text{th percentile}$ (we used $d = 3$) | Days |
| <i>CSDI</i> | Cold-spell duration indicator | Annual no. of days contributing to events in which 6 or more consecutive days experience $TN < 10\text{th percentile}$ | Days |
| <i>CSDId</i> | User-defined CSDI | Annual number of days contributing to events in which d or more consecutive days experience $TN < 10\text{th percentile}$ (we used $d = 3$) | Days |
| <i>TXgt50p</i> | Fraction of days with above-average temperature | Percentage of days on which $TX > 50\text{th percentile}$ | % |
| <i>TX95t</i> | Very-warm-day threshold | Value of 95th percentile of TX | $^{\circ}\text{C}$ |
| <i>TMge5</i> | TM of at least 5°C | No. of days on which $TM \geq 5^{\circ}\text{C}$ | Days |
| <i>TMlt5</i> | TM below 5°C | No. of days on which $TM < 5^{\circ}\text{C}$ | Days |
| <i>TMge10</i> | TM of at least 10°C | No. of days on which $TM \geq 10^{\circ}\text{C}$ | Days |
| <i>TMlt10</i> | TM below 10°C | No. of days on which $TM < 10^{\circ}\text{C}$ | Days |
| <i>TXge30</i> | TX of at least 30°C | No. of days on which $TX \geq 30^{\circ}\text{C}$ | Days |
| <i>TXge35</i> | TX of at least 35°C | No. of days on which $TX \geq 35^{\circ}\text{C}$ | Days |
| <i>TXdTNd</i> | User-defined consecutive no. of hot days and nights | Annual count of d consecutive days on which both $TX > 95\text{th percentile}$ and $TN > 95\text{th percentile}$, where $10 \geq d \geq 2$ | Events |
| <i>HDDheatn</i> | Heating degree-days | Annual sum of $n - TM$ (where n is a user-defined location-specific base temperature and $TM < n$) | Degree-days |
| <i>CDDcoldn</i> | Cooling degree-days | Annual sum of $TM - n$ (where n is a user-defined location-specific base temperature and $TM > n$; we used $n = 18^{\circ}\text{C}$) | Degree-days |
| <i>GDDgrown</i> | Growing degree-days | Annual sum of $TM - n$ (where n is a user-defined location-specific base temperature and $TM > n$) | Degree-days |
| CDD | Consecutive dry days | Max no. of consecutive dry days (when $PR < 1.0\text{ mm}$) | Days |
| R20mm | No. of very-heavy-rain days | Number of days on which $PR \geq 20\text{ mm}$ | Days |
| R95pTOT | Contribution from very wet days | $100 \times R95p/(\text{total PR})$ | % |
| R99pTOT | Contribution from extremely wet days | $100 \times R99p/(\text{total PR})$ | % |
| <i>RXdday</i> | User-defined consecutive days PR amount | Max d -day PR total (we used $d = 2$) | mm |
| SPI | Standardized precipitation index | Measure of "drought" using the SPI on time scales of 3, 6, and 12 months; see McKee et al. (1993) and WMO (2012) for further details | Unitless |
| SPEI | Standardized precipitation evapotranspiration index | Measure of drought using the SPEI on time scales of 3, 6, and 12 months; see Vicente-Serrano et al. (2010) for further details | Unitless |

TABLE 2. (Continued)

| Index codes | Indicator name | Definition | Units |
|----------------------------------|---|--|------------------------------|
| Additional indices | | | |
| <i>TXbdTNbd</i> | User-defined consecutive no. of cold days and nights | Annual no. of d consecutive days on which both $TX < 5$ th percentile and $TN < 5$ th percentile, where $10 \geq d \geq 2$ | Events |
| DTR | Daily temperature range | Mean diff between daily TX and daily TN | °C |
| TNx | Max TN | Warmest daily TN | °C |
| TXn | Min TX | Coldest daily TX | °C |
| TMm | Mean TM | Mean daily mean temperature | °C |
| TXm | Mean TX | Mean daily max temperature | °C |
| TNm | Mean TN | Mean daily min temperature | °C |
| TX10p | Amount of cool days | Percentage of time that $TX < 10$ th percentile | % |
| TX90p | Amount of hot days | Percentage of time that $TX > 90$ th percentile | % |
| TN10p | Amount of cold nights | Percentage of time that $TN < 10$ th percentile | % |
| TN90p | Amount of warm nights | Percentage of time that $TN > 90$ th percentile | % |
| CWD | Consecutive wet days | Max annual no. of consecutive wet days (when $PR \geq 1.0$ mm) | Days |
| R10mm | No. of heavy-rain days | No. of days for which $PR \geq 10$ mm | Days |
| Rnmm | No. of customized rain days | No. of days for which $PR \geq nn$ (we used $nn = 1$ mm) | Days |
| SDII | Simple daily PR intensity | Annual total PR divided by the no. of wet days (when total $PR \geq 1.0$ mm) | mm day ⁻¹ |
| R95p | Total annual PR from heavy-rain days | Annual sum of daily $PR > 95$ th percentile | mm |
| R99p | Total annual PR from very-heavy-rain days | Annual sum of daily $PR > 99$ th percentile | mm |
| Rx1day | Max 1-day PR | Max 1-day PR total | mm |
| Rx5day | Max 5-day PR | Max 5-day PR total | mm |
| <i>HWN(EHF/Tx90/Tn90)</i> | Heat wave no. as defined by the excess heat factor (EHF), 90th percentile of TX, or 90th percentile of TN | The no. of individual heat waves that occur each summer (Nov–Mar in Southern Hemisphere and May–Sep in Northern Hemisphere); a heat wave is defined as 3 or more days for which EHF is positive, $TX > 90$ th percentile of TX, or $TN > 90$ th percentile of TN, where percentiles are calculated from a user-specified base period—see Perkins and Alexander (2013) for more details on the HWN, HWF, HWD, HWM and HWA indices | Events |
| <i>HWF(EHF/Tx90/Tn90)</i> | Heat-wave frequency as defined by EHF, 90th percentile of TX, or 90th percentile of TN | The no. of days that contribute to heat waves as identified by HWN | Days |
| <i>HWD(EHF/Tx90/Tn90)</i> | Heat-wave duration as defined by EHF, 90th percentile of TX, or 90th percentile of TN | The length of the longest heat wave identified by HWN | Days |
| <i>HWM(EHF/Tx90/Tn90)</i> | Heat-wave magnitude as defined by EHF, 90th percentile of TX, or 90th percentile of TN | The mean temperature of all heat waves identified by HWN | °C (°C ² for EHF) |
| <i>HWA(EHF/Tx90/Tn90)</i> | Heat-wave amplitude as defined by EHF, 90th percentile of TX, or 90th percentile of TN | The peak daily value in the hottest heat wave (defined as the heat wave with highest HWM) | °C (°C ² for EHF) |
| <i>CWN_ECF</i> | Cold wave no. as defined by the Excess cold factor (ECF) | The no. of individual cold waves that occur each year; see Nairn and Fawcett (2015) for more details on CWN, CWF, CWD, CWM and CWA | Events |
| <i>CWF_ECF</i> | Cold-wave frequency as defined by ECF | The no. of days that contribute to cold waves as identified by CWN_ECF | Days |
| <i>CWD_ECF</i> | Cold-wave duration as defined by ECF | The length of the longest cold wave identified by CWN_ECF | Days |
| <i>CWM_ECF</i> | Cold-wave magnitude as defined by ECF | The mean temperature of all cold waves identified by CWN_ECF | °C ² |
| <i>CWA_ECF</i> | Cold-wave amplitude as defined by ECF | The min daily value in the coldest cold wave (defined as the cold wave with lowest CWM_ECF) | °C ² |

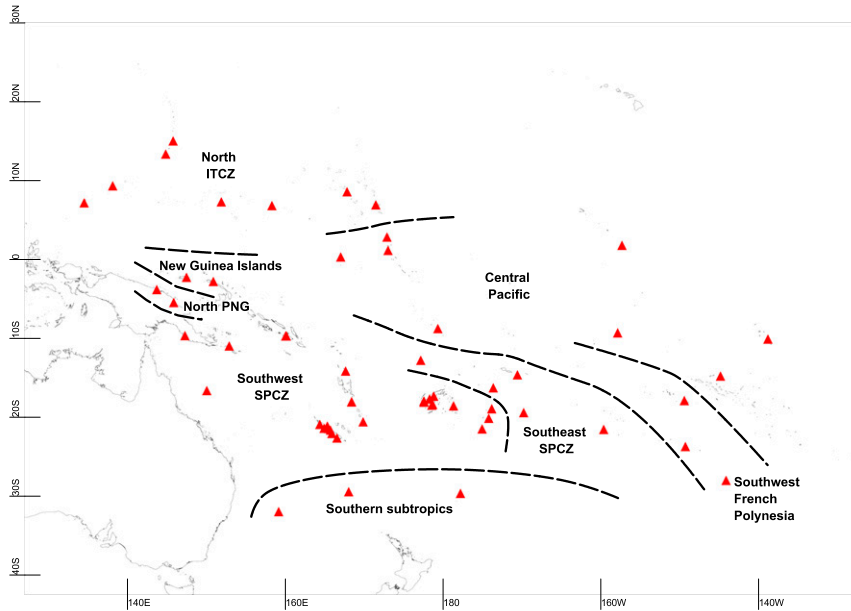


FIG. 3. Western Pacific islands coherent annual precipitation subregions as defined by cluster analysis.

significant trends even if they are absent and vice versa. Autocorrelation adjustments were incorporated in the Zhang et al. (2000) study and a number of ETCCDI associated publications (e.g., Zhang et al. 2005; Aguilar et al. 2009; Choi et al. 2009; Whan et al. 2014a).

Throughout this paper, we use the 5% level to define statistically significant trends. Only significant trends from this point forward are referred to as positive or negative.

As the stations are located over a large geographical area and unique relationships exist, especially for precipitation, with the major modes of variability including ENSO, precipitation analyses are conducted on a subregional basis (eight subregions) largely as defined by McGree et al. (2016). The exceptions are Willis Island included in the southwest SPCZ subregion and Rotuma included in the southeast SPCZ subregion. The southwest SPCZ subregion was divided into three subcomponents, namely, north Papua New Guinea (PNG), southwest SPCZ, and the southern subtropics (Fig. 3). The reclassification is based on an extension of the cluster analysis initially undertaken by McGree et al. (2016).

To account for the spatial distribution of the stations, anomalies were first calculated for each station (base period 1971–2000), and then averaged over the entire region for temperature and eight subregions for precipitation. Regional averages for individual years were calculated where less than 30% of the stations making up the region or subregion were missing. While variance adjustment has been used in similar studies in the past,

this method was found during the Whan et al. (2014a) analysis to remove interannual variability, which is undesirable. Because most of the stations have a common start and end date and the time series are relatively complete, the use of the variance adjustment method is unnecessary.

To determine whether the IPO influences trends in total and extreme temperature and precipitation, trends in the ET-SCI index with and without IPO present were compared. Trends with IPO removed that were within the 95% confidence interval of trends with IPO present were deemed not “significantly” different. To calculate the trend in the ET-SCI index with IPO removed, the strength of the relationship between 13-yr running mean TPI and the 13-yr running mean ET-SCI index was calculated using the Kendall’s tau correlation method. If significant at the 5% level, the trend in the residual of TPI and the ET-SCI index was calculated using previously described methods. Last, based on the method of Guerreiro et al. (2018) we assess changes in the magnitude of daily precipitation between 1951–82 and 1983–2015 to determine whether the most extreme precipitation events, especially those associated with typhoons/tropical cyclones have increased in recent decades. In this case, we are not interested in event attribution, only whether a statistically significant change has taken place.

Daily rainfall was ranked from highest to lowest for the complete record for each station. The largest value for the purposes of this exercise was labeled K1, the second largest value K2 and so on. K1–K20 values were

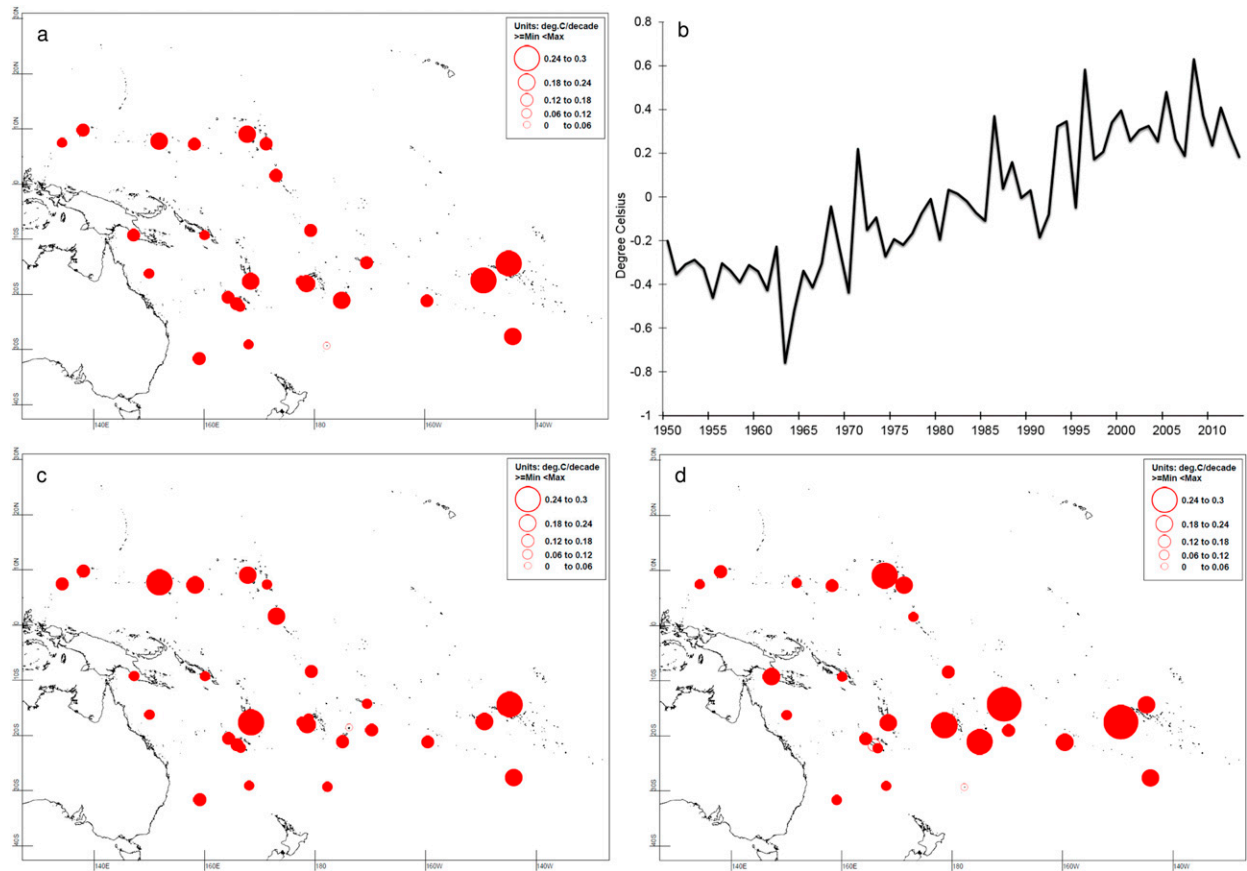


FIG. 4. Trends in annual temperature over 1951–2015 for (a) mean temperature, (c) maximum temperature, and (d) minimum temperature, along with (b) regional mean temperature anomalies relative to the 1971–2000 climatology. Solid circles represent trends significant at the 5% level. The size of the circle is proportional to the magnitude of the trend. Nonsignificant trends for Lautoka, Fiji (mean and minimum temperature), and La Foa, New Caledonia (minimum temperature), are obscured by neighboring significant trends.

assigned to bin 1, K21–K40 were assigned to bin 2, and so on until seven bins were created. The median value was then calculated for each bin. The station difference value is the median for 1983–2015 minus the median for 1951–82 for the same bin. Each station therefore had station difference values for bins 1–7. As we were interested in change associated with the highest 20 values, we used the Mann–Whitney rank-sum test (Mann and Whitney 1947) to determine whether the station difference value for bin 1 was statistically significant. The Mann–Whitney rank-sum test is a nonparametric test that uses the ranks of the sample data, instead of their specific values, to detect statistical significance. The null hypothesis is $H_0: \eta_1 = \eta_2$, the median of the first population (η_1) is equal to the median of the second population (η_2).

Further, we calculated the regional change in magnitude for each bin by averaging (mean) the station differences across the 52 stations. The Mann–Whitney rank-sum test was used again to determine whether

the difference in the regional medians for bin 1 (1951–82) and bin 1 (1983–2015) was statistically significant. This was repeated for bins 2–7.

3. Results

a. Annual and seasonal changes in mean and extreme temperatures

1) MEAN TEMPERATURE

Annual mean temperature (TM) increased at all, but two locations (Lautoka Mill and Raoul Island) in the western Pacific islands (Fig. 4). On a regional scale, annual TM warmed $0.14^{\circ}\text{C} (10 \text{ yr})^{-1}$ over 1951–2015 (Table 3; 0.91°C over 65 yr). Rates of warming were the same for December–February (DJF), March–May (MAM), and September–November (SON) [$0.14^{\circ}\text{C} (10 \text{ yr})^{-1}$]. Warming also occurs in June–August (JJA) but at a slower rate [$0.11^{\circ}\text{C} (10 \text{ yr})^{-1}$]. The TM trend

TABLE 3. Regional trends in annual and seasonal mean and extreme temperature for the western Pacific for 1951–2015 (units per 10 years). The 95% confidence intervals are shown in parentheses. Trends that are statistically significant at the 5% level are shown in italics. See Table 2 for index definitions.

| | TM (°C) | TX (°C) | TN (°C) | TNn (°C) | TNx (°C) | TXn (°C) | TXx (°C) | DTR (°C) |
|--------|--------------------------------|--------------------------------|--------------------------------|--------------------------------|--------------------------------|--------------------------------|--------------------------------|-------------------------|
| Annual | <i>+0.14</i> (+0.12, +0.16) | <i>+0.12</i> (+0.04, +0.21) | <i>+0.13</i> (+0.03, +0.23) | <i>+0.12</i> (+0.04, +0.20) | <i>+0.15</i> (+0.12, +0.18) | <i>+0.09</i> (+0.04, +0.14) | <i>+0.15</i> (+0.10, +0.20) | −0.01 (−0.02, 0.00) |
| DJF | <i>+0.14</i> (+0.12, +0.17) | <i>+0.15</i> (+0.12, +0.18) | <i>+0.14</i> (+0.12, +0.17) | <i>+0.14</i> (+0.08, +0.19) | <i>+0.16</i> (+0.07, +0.26) | <i>+0.12</i> (+0.05, +0.20) | <i>+0.14</i> (+0.10, +0.18) | +0.01 (−0.01, +0.03) |
| MAM | <i>+0.14</i> (+0.12, +0.17) | <i>+0.14</i> (+0.11, +0.16) | <i>+0.13</i> (+0.05, +0.23) | <i>+0.13</i> (+0.04, +0.21) | <i>+0.14</i> (+0.06, +0.22) | <i>+0.16</i> (+0.08, +0.24) | <i>+0.16</i> (+0.12, +0.19) | 0.00 (−0.02, +0.02) |
| JJA | <i>+0.11</i> (+0.05, +0.16) | <i>+0.10</i> (+0.04, +0.16) | <i>+0.12</i> (+0.06, +0.19) | <i>+0.15</i> (+0.07, +0.22) | <i>+0.14</i> (+0.09, +0.17) | <i>+0.11</i> (+0.05, +0.16) | <i>+0.12</i> (+0.08, +0.16) | −0.02 (−0.04, 0.00) |
| SON | <i>+0.14</i> (+0.10, +0.17) | <i>+0.12</i> (+0.04, +0.21) | <i>+0.13</i> (+0.10, +0.18) | <i>+0.13</i> (+0.06, +0.20) | <i>+0.16</i> (+0.12, +0.19) | <i>+0.14</i> (+0.07, +0.21) | <i>+0.14</i> (+0.11, +0.18) | −0.01 (−0.04, +0.01) |

over 1961–2011 [$0.15^{\circ}\text{C} (10\text{ yr})^{-1}$] was also calculated and compared with that for Whan et al. [2014a; $0.18^{\circ}\text{C} (10\text{ yr})^{-1}$, 1961–2011] and Jones et al. [2013; $0.16^{\circ}\text{C} (10\text{ yr})^{-1}$, 1961–2010]. The warmest 5 years (2010, 1998, 2007, 2013, and 2002 in descending order of TM) have occurred in the last 18 of the 65-yr study period (Fig. 4).

Warming of annual TM occurred in both halves of the study period with warming over 1983–2015 [$0.12^{\circ}\text{C} (10\text{ yr})^{-1}$] stronger than over 1951–82 [$0.09^{\circ}\text{C} (10\text{ yr})^{-1}$]. For DJF, JJA, and SON warming was stronger in the first half of the study period, whereas the opposite applies to MAM (not shown).

The annual maximum temperature (TX) trend over 1951–2015 [$0.12^{\circ}\text{C} (10\text{ yr})^{-1}$] was similar to the annual minimum temperature (TN) trend [$0.13^{\circ}\text{C} (10\text{ yr})^{-1}$; Table 3]. On a seasonal basis the strongest TX and TN warming took place in DJF, with the weakest in JJA. The annual TX trend over 1983–2015 [$0.12^{\circ}\text{C} (10\text{ yr})^{-1}$] was marginally stronger than that over 1951–82 [$0.10^{\circ}\text{C} (10\text{ yr})^{-1}$]. Trends for annual TN were also stronger over 1983–2015 [$0.12^{\circ}\text{C} (10\text{ yr})^{-1}$] when compared with 1951–82 [$0.08^{\circ}\text{C} (10\text{ yr})^{-1}$]. Spatially there was little consistency in the annual TX and TN trends, although annual TN trends were markedly stronger east of the date line (Fig. 4).

As the differences in the TX and TN trends are small, trends in annual and seasonal daily temperature range (DTR) were not statistically significant (Table 3).

2) EXTREME TEMPERATURE

All the core and additional ET-SCI temperature indices that can be calculated on a regional scale show statistically significant warming on both annual and seasonal time scales (Table 3).

On an annual scale, the amount of cold nights (TN10p) and cold days (TX10p) decreased by 1.76% and 1.70% ($10\text{ yr})^{-1}$ respectively, whereas the amount of warm nights (TN90p) and warm days (TX90p) increased by 2.28% and 2.07% ($10\text{ yr})^{-1}$, respectively. TN90p and

TX90p also show a marked increase in interannual variability from about 1988 (Fig. 5). For the four percentile-based indices, warming was strongest in DJF and lowest in JJA. These indices also show greatest warming at the upper end of the distribution. The fraction of days with above-average temperature (TXgt50p) index shows robust warming in all seasons, with the strongest warming in DJF [$5.16\% (10\text{ yr})^{-1}$]. Unlike the other percentile indices, the weakest positive trend is in SON. Warming is Southern Hemisphere dominated, as DJF is when station trends in the North Pacific are weakest (Fig. 6). It appears the weakest trends occur in the driest months of the year. For eastern Micronesia and the Marshall Islands, the driest months are January–March, whereas for a large part of the South Pacific the driest months are June–August.

The upper end of the absolute indices distribution also shows greatest warming (Table 3) with stronger increases in annual maximum TN (TNx) and maximum TX (TXx), both $0.15^{\circ}\text{C} (10\text{ yr})^{-1}$, and then decreases in the annual minimum TN (TNn) and minimum TX (TXn), 0.12° and $0.09^{\circ}\text{C} (10\text{ yr})^{-1}$, respectively.

The duration and threshold indices were not calculated at a regional level as trend calculations for some of the station-based indices do not produce meaningful results. For example, at and near the equator the mean temperature is above 25°C almost every day of the year; therefore the trends in summer days (SU) index are only viable north of 20°N and south of 20°S . For the same reason, the tropical nights (TR) index was not calculated. Where SU and TR could be calculated, most trends are positive, for example, at Lord Howe Island, where SU and TR increased by 3.7 and 4.5 days ($10\text{ yr})^{-1}$, respectively. For regional-scale TX of at least 30°C (TXge30), the subtropical stations were excluded. Like the percentile-based indices, this index shows consistent/robust annual and seasonal warming, strongest in DJF and weakest in JJA (Table 3).

TABLE 3. (Extended)

| TN10p (%) | TN90p (%) | TX10p (%) | TX90p (%) | Txgt50p (%) | TXge30 (days) | CSDId (days) | WSDId (days) | CDDcoldn (degree-days) |
|----------------|----------------|----------------|----------------|----------------|------------------|----------------|----------------|------------------------|
| -1.76 | +2.28 | -1.70 | +2.07 | +4.66 | +12.46 | -3.20 | +3.97 | +45.59 |
| (-2.08, -1.48) | (+1.91, +2.67) | (-2.00, -1.46) | (+1.72, +2.45) | (+3.94, +5.33) | (+10.64, +14.42) | (-4.09, -2.34) | (+2.78, +5.19) | (+12.99, +73.91) |
| -1.75 | +2.36 | -1.80 | +2.27 | +5.16 | +4.24 | | | |
| (-2.74, -0.78) | (+1.80, +2.90) | (-2.13, -1.48) | (+1.79, +2.87) | (+4.03, +6.53) | (+3.20, +5.01) | | | |
| -1.57 | +2.35 | -1.79 | +2.12 | +5.14 | +3.93 | | | |
| (-2.48, -0.62) | (+1.05, +3.68) | (-2.13, -1.48) | (+1.64, +2.60) | (+4.31, +6.15) | (+3.27, +4.60) | | | |
| -1.55 | +1.86 | -1.35 | +1.48 | +4.66 | +1.78 | | | |
| (-2.42, -0.71) | (+0.58, +3.16) | (-2.06, -0.74) | (+0.55, +2.44) | (+3.94, +5.33) | (+1.35, +2.18) | | | |
| -1.76 | +2.32 | -1.45 | +1.96 | +4.28 | +2.45 | | | |
| (-2.20, -1.36) | (+1.79, +2.86) | (-2.42, -0.59) | (+0.79, +3.13) | (+1.38, +7.14) | (+0.92, +4.04) | | | |

The standard warm-spell duration indicator (WSDI) index is based on the annual number of days contributing to events in which six or more consecutive days experience $TX > 90$ th percentile. The cold-spell duration indicator (CSDI) index was calculated in a similar manner. In the tropical Pacific, the number of days meeting this requirement is zero in most years, therefore for the user-specified versions a shorter period, in this case 3 days, was used. On a regional scale, CSDI3 decreased by 3.20 days $(10\text{ yr})^{-1}$ and WSDI3 increased by 3.97 days $(10\text{ yr})^{-1}$.

Because air conditioning is frequently used in the tropical and subtropical Pacific, especially in the summer months, the ET-SCI cooling degree-days (CDDcoldn) index is important. A positive trend of 45.59 degree-days $(10\text{ yr})^{-1}$ is derived on a regional scale suggesting that demand for air conditioning (and therefore electricity demand) has increased significantly over the last 65 yr.

Several core and additional ET-SCI indices were not analyzed because the time series were unusable; this was the case for the entire or part of a region. These indices have been presented in italics in Table 2. The number and frequency of heat waves and cold waves in the tropical Pacific was zero for many years; therefore, heat-wave and cold-wave duration, magnitude, and amplitude could not be calculated. At Alofi-Hanan Airport on Niue, for example, there were 19 such annual cases for heat-wave number (HWN) (TX90) in 65 yr, somewhat equally spread across the record, with a further 18 cases of one annual heat-wave event. This is likely to be due to the low day-to-day temperature variability on oceanic islands. Although there are statistical methods that account for large numbers of zero values in a time series (e.g., zero inflation models), they have not been used in this study because a standardized method for trend calculation is preferred. The limitations of indices

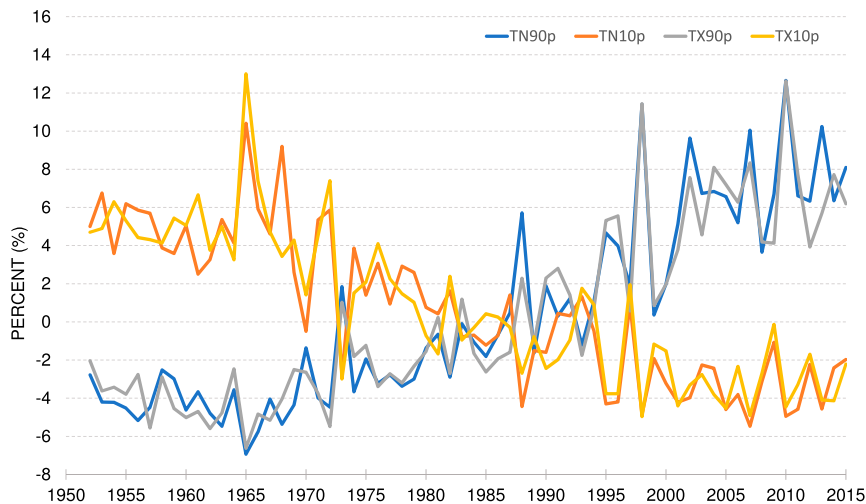


FIG. 5. Regional amount of warm nights (TN90p), cold nights (TN10p), hot days (TX90p), and cool days (TX10p) anomalies relative to the 1971–2000 climatology.

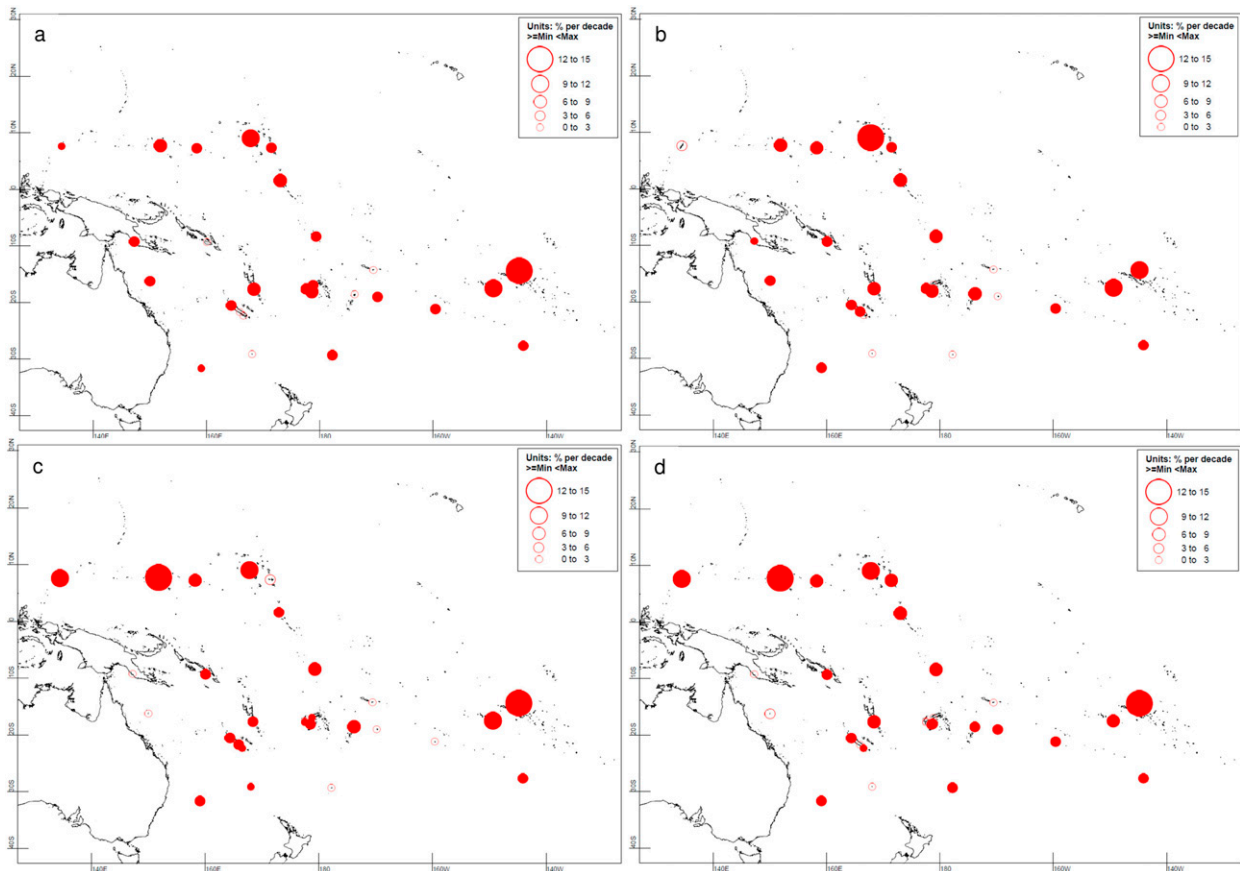


FIG. 6. Trends in the fraction of days with above-average temperature (TXgt50p) over 1951–2015 for (a) DJF, (b) MAM, (c) JJA, and (d) SON. Solid circles represent trends significant at the 5% level. The size of the circle is proportional to the magnitude of the trend.

in detecting heat-wave events is well known and is discussed in detail in Perkins (2015) and Perkins and Alexander (2013).

b. Annual and seasonal changes in total and extreme precipitation

1) TOTAL PRECIPITATION

Of the eight Pacific subregions, only the southern subtropics and southwest French Polynesia showed statistically significant annual total precipitation (PR) trends; both of which were negative (Table 4). These were associated with negative trends in JJA in the former and in DJF in the latter. Significant negative trends were also present in SON in the north ITCZ and north PNG subregions (Table 4).

Although not associated with statistically significant trends, the annual (not shown), MAM, SON, and, to a lesser extent, DJF maps show an El Niño-like pattern in which the ITCZ is displaced south toward the equator

and the SPCZ is displaced northeast toward the central Pacific (Fig. 7).

2) EXTREME PRECIPITATION

Similar to total PR, the proportion of statistically significant extreme precipitation indices trends was small. Significant trends were predominately negative and were by and large located in the southern subtropics and southwest French Polynesia subregions (Tables 4 and 5).

In the case of southwest French Polynesia, there was a decrease in moderate- to high-intensity precipitation events, especially those experienced over multiple days. For the duration absolute indices (Rx1day, Rx2day, and Rx5day), the negative trends occurred in DJF, whereas for R10mm the negative trends occurred in SON and those for R20mm occurred in MAM. Declines are also present in the percentile-based (R95p, R95pTOT, R99p, and R99pTOT) and daily PR intensity (SDII) indices. These negative trends contributed to an increase in

TABLE 4. Subregional trends for total and extreme precipitation for 1951–2015 (units per 10 years). The 95% confidence intervals are shown in parentheses. Trends that are statistically significant at the 5% level are shown in italics. NA indicates that the trend is not available because of insufficient data. See Table 2 for index definitions.

| | Total PR (mm) | Rx1day (mm) | Rx2day (mm) | Rx5day (mm) | R1mm (days) | R10mm (days) | R20mm (days) | CDD (days) | CWD (days) |
|----------------------------|-----------------------|----------------------|------------------------|------------------------|----------------------|----------------------|----------------------|----------------------|----------------------|
| Central Pacific | | | | | | | | | |
| Annual | +28.4 (-71.5, +132.7) | +3.71 (+0.28, +7.85) | +5.76 (-2.99, +14.19) | +4.73 (-2.54, +12.50) | +1.46 (-1.91, +5.06) | +0.67 (-1.99, +3.15) | +0.53 (-1.27, +2.20) | -1.83 (-3.45, -0.08) | +0.30 (-0.91, +1.52) |
| DJF | -9.5 (-47.2, +26.5) | +1.95 (-1.57, +5.52) | +1.01 (-8.45, +8.59) | +0.88 (-6.65, +8.44) | +0.34 (-0.99, +1.62) | -0.05 (-0.84, +0.69) | +0.02 (-0.56, +0.55) | -0.24 (-1.26, +0.62) | +0.20 (-0.48, +0.77) |
| MAM | +17.2 (-15.0, +45.5) | +2.69 (-0.83, +6.00) | +7.42 (+1.34, +13.67) | +5.18 (-0.67, +10.56) | +0.83 (-0.10, +1.72) | +0.56 (-0.16, +1.23) | +0.28 (-0.23, +0.75) | -0.63 (-1.23, +0.02) | +0.31 (-0.24, +0.82) |
| JJA | +3.1 (-17.5, +20.2) | +0.67 (-1.72, +3.39) | +0.58 (-5.64, +5.86) | +1.11 (-5.28, +5.43) | +0.16 (-0.60, +0.89) | -0.09 (-0.58, +0.46) | 0.00 (-0.35, +0.34) | -0.01 (-0.53, +0.51) | +0.23 (-0.12, +0.57) |
| SON | +11.5 (-9.1, +33.6) | +2.26 (-0.62, +5.15) | +2.31 (-2.78, +8.05) | -1.63 (-8.96, +5.86) | +0.61 (-0.28, +1.44) | +0.19 (-0.41, +0.73) | +0.16 (-0.18, +0.47) | -0.61 (-1.36, +0.24) | +0.27 (-0.16, +0.63) |
| New Guinea Islands | | | | | | | | | |
| Annual | +4.0 (-102.4, +110.2) | -0.78 (-5.33, +3.44) | -1.78 (-10.92, +5.96) | -1.63 (-8.96, +5.86) | -0.28 (-5.49, +4.78) | +0.47 (-2.71, +3.81) | +1.06 (-1.57, +3.57) | +0.42 (-1.06, +1.96) | -1.49 (-3.04, -0.19) |
| DJF | -12.5 (-42.9, +16.1) | -3.23 (-6.75, +0.50) | -1.04 (-7.76, +5.95) | +0.74 (-5.67, +6.56) | -0.58 (-1.89, +0.83) | -0.47 (-1.47, +0.63) | 0.00 (-0.63, +0.74) | +0.01 (-0.89, +0.85) | -0.66 (-1.55, +0.32) |
| MAM | +3.9 (-20.0, +26.2) | -1.47 (-4.62, +1.08) | -0.58 (-5.20, +3.97) | -2.00 (-5.88, +1.21) | -0.97 (-2.30, +0.29) | -0.03 (-0.92, +0.83) | +0.07 (-0.51, +0.61) | +0.40 (-0.39, +1.16) | -1.17 (-2.10, -0.27) |
| JJA | +26.7 (-13.6, +66.2) | +2.00 (-2.10, +6.29) | +11.42 (+1.20, +20.95) | +8.06 (-0.44, +16.02) | 0.00 (-1.35, +1.86) | +0.83 (-0.15, +1.88) | +0.63 (-0.14, +1.43) | +0.15 (-0.53, +0.83) | +0.23 (-0.69, +1.15) |
| SON | -3.2 (-50.9, +34.8) | +0.11 (-3.83, +3.54) | -3.00 (-9.13, +3.78) | -3.00 (-8.53, +2.35) | +0.12 (-2.10, +2.05) | +0.01 (-1.18, +1.21) | +0.10 (-0.76, +0.97) | +0.19 (-0.74, +1.09) | +0.23 (-0.82, +1.12) |
| North ITCZ | | | | | | | | | |
| Annual | -37.3 (-77.1, +6.6) | -0.62 (-5.06, +3.57) | -1.00 (-7.66, +5.24) | -0.46 (-5.81, +6.11) | -1.36 (-3.15, +0.80) | -1.08 (-2.44, +0.55) | -0.71 (-1.69, +0.26) | +0.42 (-0.52, +1.42) | -0.79 (-2.19, +0.60) |
| DJF | -3.1 (-21.5, +17.2) | -0.82 (-3.04, +1.70) | -3.91 (-8.70, +0.20) | -3.69 (-8.26, +0.55) | +0.24 (-2.56, +1.05) | +0.13 (-0.50, +0.67) | 0.00 (-0.35, +0.38) | -0.33 (-0.75, +0.13) | -0.15 (-0.65, +0.35) |
| MAM | -13.9 (-39.0, +10.4) | -1.44 (-4.61, +2.43) | -4.11 (-10.58, +3.15) | -2.73 (-8.42, +3.00) | -0.23 (-1.22, +0.65) | -0.33 (-1.02, +0.39) | -0.19 (-0.67, +0.23) | -0.11 (-0.61, +0.45) | -0.23 (-0.82, +0.31) |
| JJA | -2.3 (-23.0, +16.3) | +0.68 (-1.88, +3.23) | +1.49 (-4.76, +7.43) | +0.91 (-4.66, +6.50) | -0.44 (-0.97, 0.00) | -0.15 (-0.59, +0.24) | -0.13 (-0.45, +0.16) | +0.22 (+0.02, +0.42) | -0.06 (-0.54, +0.37) |
| SON | -14.1 (-28.7, -0.3) | -0.61 (-2.78, +1.55) | -1.01 (-0.37, +3.54) | -0.13 (-3.60, +3.42) | -0.36 (-0.98, +0.26) | -0.31 (-0.82, +0.18) | -0.37 (-0.58, 0.00) | +0.23 (0.00, +0.50) | -0.45 (-0.99, +0.11) |
| North PNG | | | | | | | | | |
| Annual | -21.8 (-121.8, +92.3) | -2.06 (-6.08, +2.10) | -1.23 (-10.73, +6.42) | +0.69 (-4.40, +4.06) | 0.00 (-1.14, +0.83) | 0.00 (-0.63, +0.56) | -0.17 (-0.65, +0.38) | NA | NA |
| DJF | -10.0 (-30.8, +12.0) | +0.71 (-3.86, +6.07) | +0.50 (-6.38, +6.28) | -2.41 (-7.70, +2.52) | -0.08 (-1.70, +1.50) | +0.41 (-0.81, +1.53) | +0.25 (-0.37, +0.82) | +0.27 (-0.81, +1.24) | 0.00 (-0.67, +0.50) |
| MAM | +17.5 (-12.9, +55.3) | -1.48 (-4.76, +2.29) | -1.31 (-7.55, +5.25) | +2.17 (-4.08, +8.23) | NA | NA | NA | -0.04 (-0.82, +0.61) | -0.16 (-0.93, +0.60) |
| JJA | -9.9 (-48.6, +33.2) | NA | +1.30 (-6.89, +8.78) | -8.83 (-14.75, -4.38) | NA | NA | NA | 0.00 (-0.77, +1.19) | NA |
| SON | -26.7 (-53.6, -0.9) | -3.00 (-6.38, +0.15) | -9.89 (-17.05, -3.88) | -0.98 (-6.38, +0.15) | -1.10 (-2.69, +0.33) | -0.64 (-1.60, +0.36) | -0.48 (-1.18, 0.00) | +0.51 (-0.79, +1.90) | -0.32 (-0.97, +0.29) |
| Southeast SPZC | | | | | | | | | |
| Annual | -19.0 (-66.7, +25.4) | +0.68 (-3.09, +4.41) | +1.63 (-4.15, +7.58) | +2.41 (-2.89, +7.95) | +0.61 (-1.11, +2.35) | -0.26 (-1.46, +0.95) | +0.12 (-0.60, +0.75) | -0.03 (-1.25, +1.30) | -0.10 (-0.85, +0.62) |
| DJF | -4.8 (-25.0, +16.3) | -0.71 (-4.70, +3.06) | -2.11 (-10.89, +5.23) | -4.16 (-10.30, +3.05) | +0.27 (-0.60, +1.08) | +0.09 (-0.54, +0.69) | 0.00 (-0.33, +0.41) | +0.09 (-0.48, +0.60) | +0.08 (-0.45, +0.57) |
| MAM | +3.2 (-12.0, +18.4) | -0.71 (-3.34, +2.19) | -3.40 (-9.33, +2.89) | -3.65 (-9.38, +1.71) | -0.25 (-0.86, +0.46) | -0.27 (-0.86, +0.24) | -0.27 (-0.63, +0.12) | +0.10 (0.24, +0.49) | -0.18 (0.60, +0.18) |
| JJA | -11.0 (30.4, +8.3) | -0.17 (2.89, +2.33) | +0.92 (-4.30, +6.22) | +1.44 (-3.06, +5.78) | +0.35 (-0.34, +0.94) | +0.12 (-0.30, +0.54) | +0.08 (-0.18, +0.35) | -0.19 (-0.69, +0.35) | 0.00 (-0.33, +0.34) |
| SON | -3.3 (-20.0, +12.9) | -1.12 (-4.12, +1.88) | -1.04 (-7.14, +5.10) | -1.20 (-5.89, +3.56) | -0.04 (-0.72, +0.80) | 0.00 (-0.45, +0.39) | +0.02 (-0.25, +0.33) | +0.02 (-0.73, +0.70) | -0.04 (-0.36, +0.31) |
| Southern subtropics | | | | | | | | | |
| Annual | -33.6 (-63.4, -1.9) | -1.50 (-5.31, +1.83) | -2.17 (-7.11, +3.77) | -1.21 (-6.03, +4.00) | -1.91 (-3.33, -0.37) | -0.87 (-1.67, -0.11) | -0.54 (-1.11, 0.00) | +1.43 (0.00, +2.93) | -0.97 (-1.76, -0.12) |
| DJF | -5.0 (-20.0, +10.3) | -1.09 (-5.14, +2.72) | -3.28 (-9.67, +3.74) | -3.24 (-9.19, +3.73) | 0.00 (-0.51, +0.65) | -0.12 (-0.38, +0.14) | 0.00 (-0.26, +0.14) | +0.16 (-0.59, +0.90) | 0.00 (-0.29, +0.27) |
| MAM | +1.1 (-13.0, +13.1) | -1.43 (-4.77, +1.62) | -1.38 (-6.25, +3.66) | -0.52 (-5.64, +4.03) | -0.16 (-0.88, +0.60) | +0.07 (-0.20, +0.40) | 0.00 (-0.16, +0.28) | +0.01 (-0.68, +0.66) | +0.09 (-0.19, +0.38) |
| JJA | -18.1 (-30.2, -6.5) | -1.97 (-4.43, +0.24) | -4.28 (-8.33, -0.24) | -2.92 (-6.50, +0.45) | -1.09 (-1.67, -0.47) | -0.51 (-0.83, -0.13) | -0.22 (-0.44, 0.00) | +0.25 (0.00, +0.58) | -0.60 (-1.08, -0.23) |
| SON | -7.1 (-18.8, +3.4) | -0.51 (-3.41, +2.29) | -0.98 (-5.31, +2.96) | -1.13 (-4.20, +2.79) | -0.49 (-1.09, 0.00) | -0.21 (-0.56, +0.10) | -0.16 (-0.38, 0.00) | +0.54 (0.00, +1.00) | -0.26 (-0.51, 0.00) |
| Southwest French Polynesia | | | | | | | | | |
| Annual | -53.4 (-99.3, -8.9) | -3.50 (-7.31, +0.04) | -14.19 (-22.98, -4.67) | -9.18 (-18.09, -1.69) | +1.29 (-0.58, +2.87) | -1.43 (-2.37, -0.32) | -1.12 (-2.04, -0.31) | -1.62 (-3.53, +0.66) | -0.04 (-0.94, +0.77) |
| DJF | -23.4 (-46.0, -3.1) | -4.78 (-8.29, -1.42) | -13.50 (-22.27, -5.93) | -10.62 (-20.02, -2.28) | +0.18 (-0.60, +1.00) | -0.49 (-1.09, +0.01) | -0.27 (-0.72, +0.10) | -0.15 (-0.78, +0.40) | -0.39 (-0.81, -0.06) |
| MAM | -16.4 (-35.7, +5.0) | -1.97 (-5.62, +1.41) | -5.08 (-11.25, +3.31) | -5.11 (-12.31, +2.33) | +0.48 (-0.33, +1.17) | -0.38 (-0.89, +0.10) | -0.46 (-0.88, -0.07) | +0.06 (-0.78, +0.83) | +0.18 (-0.28, +0.64) |
| JJA | -3.5 (-16.2, +8.1) | -1.84 (-4.78, +1.51) | -4.83 (-11.71, +2.49) | -6.02 (-12.72, +1.14) | +0.71 (+0.17, +1.33) | 0.00 (-0.37, +0.31) | -0.15 (-0.41, +0.09) | -0.91 (-1.54, -0.24) | +0.28 (-0.05, +0.57) |
| SON | -13.0 (-31.3, +4.7) | -0.31 (-3.50, +2.77) | -3.66 (-9.33, +1.59) | -2.61 (-8.35, +1.85) | +0.03 (-0.70, +0.81) | -0.40 (-0.80, -0.01) | -0.26 (-0.58, +0.02) | -0.77 (-1.53, -0.01) | +0.06 (-0.32, +0.39) |
| Southwest SPZC | | | | | | | | | |
| Annual | -12.7 (-77.2, +56.0) | -0.14 (-3.05, +3.07) | -1.56 (-8.71, +4.37) | -1.21 (-7.22, +4.48) | +0.52 (-2.30, +3.31) | -0.33 (-2.11, +1.43) | -0.25 (-1.37, +0.94) | -0.54 (-2.50, +1.67) | -0.10 (-0.65, +0.48) |
| DJF | +4.7 (-22.8, +27.8) | +0.51 (-3.21, +4.26) | -1.00 (-8.02, +5.46) | -1.00 (-7.78, +6.05) | +0.15 (-0.78, +1.03) | +0.10 (-0.55, +0.66) | +0.10 (-0.35, +0.46) | -0.27 (-0.99, +0.37) | -0.01 (-0.44, +0.41) |
| MAM | +0.9 (-19.1, +19.2) | +0.59 (-2.15, +3.14) | -2.07 (-8.60, +3.47) | -1.87 (-7.42, +3.70) | +0.37 (-0.30, +1.08) | -0.01 (-0.42, +0.49) | -0.03 (-0.37, +0.28) | -0.25 (-0.89, +0.20) | 0.00 (-0.25, +0.19) |
| JJA | -4.3 (-15.0, +7.6) | -0.59 (-2.49, +1.30) | -1.28 (-6.09, +3.55) | -1.46 (-5.69, +2.88) | +0.17 (-0.35, +0.68) | -0.05 (-0.32, +0.28) | -0.05 (-0.27, +0.16) | -0.36 (-1.10, +0.42) | -0.01 (-0.26, +0.32) |
| SON | -9.7 (-33.2, +13.3) | -2.59 (-5.23, +0.33) | -4.34 (-9.37, +1.49) | -4.35 (-8.93, +0.69) | -0.28 (-1.42, +0.79) | -0.26 (-0.84, +0.39) | -0.20 (-0.55, +0.20) | +0.64 (-0.57, +1.88) | -0.04 (-0.39, +0.30) |

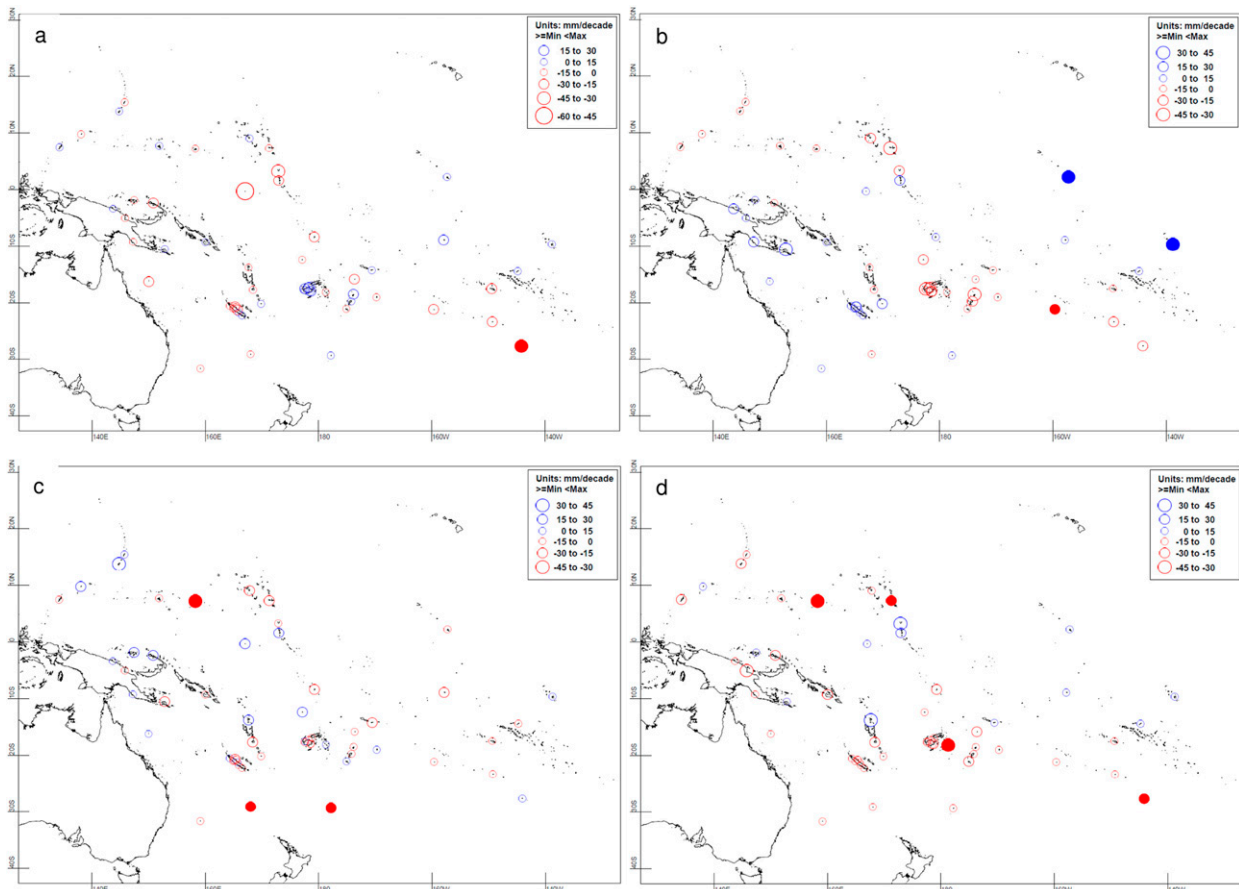


FIG. 7. Trends in total precipitation over 1951–2015 for (a) DJF, (b) MAM, (c) JJA, and (d) SON. Blue circles represent positive trends, and red circles show negative trends. Solid circles represent trends significant at the 5% level. The size of the circle is proportional to the magnitude of the trend.

meteorological drought [standardized precipitation index (SPI) (SPI-3 for February and SPI-6 for April; Table 6) over the extended summer. On the other hand, there was an increase in the number of rain days (R1mm) and a decrease in the number of consecutive dry days (CDD) in JJA (Table 4).

The southern subtropics showed a similar drying pattern but from different underlying causes: the negative trend in annual total PR was associated with declines in R1mm, R10mm, and consecutive wet days (CWD) and an increase in CDD. In other words, a decrease in low- to moderate-intensity precipitation events was observed. On a seasonal scale, there were negative trends in JJA total PR, R1mm, R10mm, CWD, and Rx2day, and for SON, a positive trend in CDD and a negative trend in CWD. The southern subtropics drying trend in JJA and SON was also apparent in the drought indices, for which negative trends were observed for SPI-3 for August, standardized precipitation evaporation index 3 (SPEI-3) for August, SPI-6 for October, SPEI-6 for October,

SPI-12 for December, and SPEI-12 for December (Tables 6 and 7; Fig. 8). Unlike the southwest French Polynesia subregion, the drying trend in the southern subtropics was present in both the precipitation (SPI) and evapotranspiration drought (SPEI) indices.

In the central Pacific there was a decrease in CDD and an increase in annual Rx1day and MAM Rx2day. In the north ITCZ and north PNG subregions, negative trends in SON total PR were associated with declines in SON R20mm and an increase in drought (SPEI-3 for November and SPEI-6 for October) for the former, and with declines in Rx2day and Rx5day in the latter (Tables 2 and 3). There were no significant total or extreme precipitation trends in the southwest and southeast SPCZ subregions.

While some indices displayed significant trends on a subregional level (Tables 4 and 5), the same did not apply at a station level. None of the station trends for annual Rx1day, Rx2day, and Rx5day, for example, were statistically significant (not shown).

TABLE 5. Subregional trends for annual total and extreme precipitation, also expressed as percentile based and as daily PR intensity (SDII) for 1951–2015 (units per 10 years). The 95% confidence intervals are shown in parentheses. Trends that are statistically significant at the 5% level are shown in italics. NA indicates that the trend is not available because of insufficient data. See Table 2. for index definitions.

| | R95p (mm) | R95pTOT (%) | R99p (mm) | R99pTOT (%) | SDII (mm day ⁻¹) |
|----------------------------|-------------------------|----------------------|-------------------------|----------------------|------------------------------|
| Central Pacific | +12.55 (−25.80, +56.52) | +0.56 (−0.60, +1.83) | +11.99 (−3.56, +27.24) | +0.56 (−0.06, +1.19) | +0.11 (−0.21, +0.48) |
| New Guinea Islands | +20.13 (−29.15, +66.36) | +0.34 (−0.47, +1.16) | −5.30 (−34.44, +25.34) | −0.21 (−1.07, +0.52) | +0.19 (−0.05, +0.42) |
| North ITCZ | −15.37 (−44.23, +16.15) | −0.18 (−0.90, +0.60) | −2.56 (−18.40, +16.47) | +0.07 (−1.27, +0.58) | −0.08 (−0.22, +0.06) |
| North PNG | −16.13 (−66.68, +30.21) | NA | −20.30 (−43.36, +7.63) | −0.34 (−0.75, +0.31) | +0.03 (−0.26, +0.30) |
| Southeast SPCZ | −11.34 (−38.88, +15.09) | −0.30 (−1.02, +0.37) | −6.72 (−22.02, +9.08) | −0.27 (−0.75, +0.31) | −0.14 (−0.39, +0.08) |
| Southern subtropics | −18.26 (−37.82, +2.44) | −0.58 (−1.44, +0.28) | −4.70 (−15.33, +5.67) | −0.11 (−0.79, +0.51) | −0.13 (−0.29, +0.03) |
| Southwest French Polynesia | −49.33 (−73.65, −21.19) | −1.52 (−2.24, −0.62) | −26.15 (−41.55, −10.30) | −1.03 (−1.65, −0.38) | −0.66 (−0.93, −0.37) |
| Southwest SPCZ | −7.73 (−32.69, +20.58) | −0.09 (−0.64, +0.40) | −1.03 (−9.81, +11.05) | −0.01 (−0.43, +0.42) | −0.16 (−0.39, +0.07) |

c. IPO influence on temperature and precipitation trends

Over the period 1951–2015, trends in the annual and seasonal TPI for the IPO were nonsignificant.

Apart from TNn (JJA), TNx (MAM), TXx (MAM, SON), and DTR (annual, MAM, SON) the relationships between the mean and extreme temperature indices and the TPI were nonsignificant. Trends in the temperature indices with IPO removed (not presented) were within $0.02^{\circ}\text{C} (10\text{ yr})^{-1}$ of the trends with IPO present and therefore within the 95% confidence interval of the trends with IPO.

The IPO relationship with total and extreme precipitation varies across the region (strongest closest to the equator) and by season. Where the relationship was statistically significant, the differences in trends in precipitation with IPO and without IPO were small and within the 95% confidence interval of the trends with IPO. In some cases, statistically significant trends became nonsignificant and vice versa but only in cases where trends in precipitation with IPO were marginally significant.

d. Changes in magnitude of the most extreme daily precipitation values

On a station scale, the bin-1 (K1–K20) difference values (1983–2015 median minus 1951–82 median) show significant variability across the region (Fig. 9). Of those that were statistically significant, most showed increases (8 of 11). Six of the eight locations were in the western

and central Pacific and within 10° of the equator. If the *p* value is increased to 10%, five additional stations in the southwestern Pacific region show positive differences.

None of the regional-scale differences in the median values (bins 1–7) for 1951–82 and 1983–2015 were statistically significant. Figure 10 shows that on a station scale the magnitudes of increases were also on average greater than magnitudes of decreases.

4. Discussion and conclusions

There is a general perception among Pacific island communities that changes in weather and climate are occurring in their region. More change is believed to have occurred in the past decade than at any other time in the past. Local perceptions of climate change in their countries include: shifts in seasonal patterns of rainfall and tropical cyclones, more frequent and extreme rainfall causing flooding and mudslides, more drought and fires, and more hot days (Australian Bureau of Meteorology and CSIRO 2011a,b).

Changes in mean and extreme temperature documented here are consistent with these perceptions. On a regional scale, we found annual mean temperature increased by $0.14^{\circ}\text{C} (10\text{ yr})^{-1}$. Trends over 1961–2011 [$0.15^{\circ}\text{C} (10\text{ yr})^{-1}$] were also calculated and compared with that for Whan et al. [2014a; $0.18^{\circ}\text{C} (10\text{ yr})^{-1}$, 1961–2011] and Jones et al. [(2013; $0.16^{\circ}\text{C} (10\text{ yr})^{-1}$, 1961–2010]. Data rescue efforts in recent years, station selection, and a weaker positive trend in the last decade (akin to that in the first 15–20 yr) are likely responsible for the variance. Increases in mean

TABLE 6. Subregional drought-indices trends for 1951–2015 (units per 10 years). The 95% confidence intervals are shown in parentheses. Trends that are statistically significant at the 5% level are shown in italics. See Table 2 for index definitions.

| | SPI-3 Aug | SPI-3 Feb | SPI-3 May | SPI-3 Nov | SPI-6 Apr | SPI-6 Oct | SPI-12 Dec | SPI-12 Jun |
|---------------------|----------------------|----------------------|----------------------|----------------------|----------------------|----------------------|----------------------|----------------------|
| Central Pacific | 0.00 (−0.08, +0.08) | 0.00 (−0.10, +0.11) | +0.08 (−0.01, +0.17) | +0.06 (−0.03, +0.14) | +0.03 (−0.07, +0.12) | +0.02 (−0.08, +0.13) | +0.03 (−0.09, +0.13) | +0.03 (−0.09, +0.14) |
| New Guinea | +0.15 (−0.01, +0.31) | −0.03 (−0.20, +0.14) | +0.01 (−0.12, +0.15) | +0.04 (−0.20, +0.24) | −0.04 (−0.20, +0.10) | +0.15 (−0.03, +0.36) | +0.07 (−0.15, +0.31) | +0.12 (−0.15, +0.37) |
| Islands | | | | | | | | |
| North ITCZ | −0.01 (−0.09, +0.09) | 0.00 (−0.08, +0.07) | −0.03 (−0.12, +0.04) | −0.05 (−0.13, +0.02) | −0.03 (−0.12, +0.05) | −0.03 (−0.12, +0.07) | −0.04 (−0.12, +0.04) | −0.03 (−0.13, +0.06) |
| North PNG | +0.03 (−0.16, +0.25) | 0.00 (−0.15, +0.13) | +0.08 (−0.15, +0.28) | −0.08 (−0.20, +0.03) | +0.01 (−0.19, +0.21) | −0.05 (−0.18, +0.12) | −0.01 (−0.21, +0.19) | +0.01 (−0.20, +0.20) |
| Southeast | +0.01 (−0.09, +0.10) | −0.02 (−0.11, +0.07) | −0.05 (−0.13, +0.02) | −0.02 (−0.10, +0.05) | −0.09 (−0.18, +0.01) | −0.01 (−0.10, +0.08) | −0.05 (−0.14, +0.05) | −0.05 (−0.15, +0.05) |
| SPCZ | | | | | | | | |
| Southern subtropics | −0.16 (−0.26, −0.06) | −0.02 (−0.10, +0.05) | 0.00 (−0.10, +0.09) | −0.06 (−0.16, +0.03) | +0.02 (−0.06, +0.10) | −0.18 (−0.30, −0.07) | −0.10 (−0.18, 0.00) | −0.08 (−0.20, +0.02) |
| French Polynesia | −0.02 (−0.15, +0.09) | −0.10 (−0.20, 0.00) | −0.08 (−0.16, +0.01) | −0.09 (−0.20, +0.02) | −0.09 (−0.19, −0.01) | −0.05 (−0.21, +0.08) | −0.14 (−0.28, −0.02) | −0.14 (−0.25, −0.03) |
| Southwest SPCZ | −0.03 (−0.12, +0.05) | +0.02 (−0.07, +0.09) | 0.00 (−0.07, +0.08) | −0.07 (−0.18, +0.04) | −0.02 (−0.12, +0.07) | −0.01 (−0.12, +0.08) | −0.03 (−0.16, +0.09) | −0.03 (−0.14, +0.08) |

TABLE 7. Additional subregional drought-indices trends for 1951–2015 (units per 10 years). The 95% confidence intervals are shown in parentheses. Trends that are statistically significant at the 5% level are shown in italics. See Table 2 for index definitions.

| | SPEI-3 Aug | SPEI-3 Feb | SPEI-3 May | SPEI-3 Nov | SPEI-6 Apr | SPEI-6 Oct | SPEI-12 Dec | SPEI-12 Jun |
|---------------------|----------------------|----------------------|----------------------|----------------------|----------------------|----------------------|----------------------|----------------------|
| Central Pacific | −0.04 (−0.13, +0.03) | −0.03 (−0.17, +0.07) | +0.02 (−0.10, +0.14) | 0.00 (−0.09, +0.08) | −0.02 (−0.14, +0.09) | −0.03 (−0.14, +0.06) | −0.02 (−0.15, +0.10) | −0.10 (−0.19, +0.05) |
| North ITCZ | −0.07 (−0.16, +0.02) | 0.00 (−0.09, +0.09) | −0.05 (−0.15, +0.04) | −0.09 (−0.18, 0.00) | −0.01 (−0.10, +0.09) | −0.10 (−0.22, −0.01) | −0.09 (−0.17, +0.01) | −0.07 (−0.17, +0.03) |
| Southeast | 0.00 (−0.12, +0.12) | 0.00 (−0.09, +0.09) | −0.04 (−0.14, +0.06) | 0.00 (−0.09, +0.09) | −0.07 (−0.14, +0.08) | −0.02 (−0.12, +0.09) | −0.02 (−0.12, +0.09) | −0.05 (−0.17, +0.08) |
| SPCZ | | | | | | | | |
| Southern subtropics | −0.16 (−0.26, −0.06) | −0.04 (−0.13, +0.04) | −0.01 (−0.10, +0.09) | −0.09 (−0.20, +0.01) | +0.02 (−0.08, +0.10) | −0.21 (−0.21, −0.02) | −0.11 (−0.21, −0.02) | −0.10 (−0.23, 0.00) |
| French Polynesia | −0.07 (−0.18, +0.04) | −0.10 (−0.21, +0.02) | −0.07 (−0.21, +0.08) | −0.10 (−0.24, +0.05) | −0.10 (−0.23, +0.04) | −0.09 (−0.24, +0.05) | −0.18 (−0.37, +0.01) | −0.10 (−0.26, +0.05) |
| Southwest SPCZ | −0.04 (−0.13, +0.05) | +0.01 (−0.08, +0.10) | −0.02 (−0.11, +0.06) | −0.09 (−0.20, +0.04) | −0.03 (−0.11, +0.06) | −0.03 (−0.13, +0.08) | −0.06 (−0.18, +0.06) | −0.05 (−0.15, +0.06) |

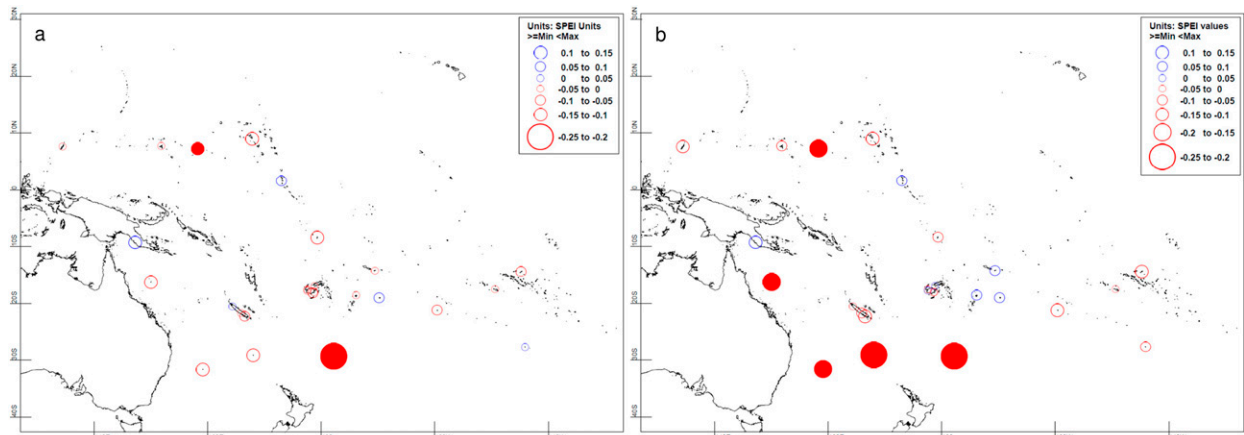


FIG. 8. Trends in drought over 1951–2015: (a) SPEI-3 for August and (b) SPEI-6 for October. Red or blue circles represent an increase or decrease in drought conditions, respectively. Solid circles represent trends that are significant at the 5% level. The size of the circle is proportional to the magnitude of the trend.

temperature occurred in all seasons and in both halves of the 1951–2015 study period.

At a regional scale, increases in annual mean maximum and minimum temperature were similar in terms of the rates of increase. Spatially there was little consistency in the annual maximum and minimum temperature trends, although annual minimum temperature trends were markedly stronger east of the date line. Whether this is a climate phenomenon or the result of unresolved inhomogeneities is unclear. Strong annual mean temperature trends were also present east of the date line in Jones et al. (2013) and Whan et al. (2014a).

The ET-SCI indices showed strong warming on a regional scale in all seasons. For the percentile-based and absolute indices, the warming was strongest in DJF and lowest in JJA. Both sets of indices showed greatest warming at the upper end of the distribution. According to Whan et al. (2014a) this a recent phenomenon with the reverse occurring in earlier decades.

A noteworthy feature of the new ET-SCI indices is their relevance to industry. The cooling degree-days index (CDDcoldn) for example showed a regional-scale positive trend of 45.59 degree-days $(10\text{ yr})^{-1}$. This suggests electricity demand due to warming alone may have doubled since 1951. Increase in demand is likely to be even greater when taking into consideration population growth. Noting that in several countries there is limited access to electricity beyond the major towns and cities, and the average income is lower than in the western world, it is likely many Pacific Islanders, especially the elderly, are unable to afford adequate cooling. Higher-than-normal summer temperatures therefore pose a greater health risk now than they did in the past. Karl and Knight (1997) found that increases in warm nights

can contribute substantially to heat-wave mortality where air conditioning is uncommon, as the human body depends upon nighttime temperatures to cool.

The results of our temperature analyses are largely consistent with global (Alexander et al. 2006), neighboring (Choi et al. 2009; Caesar et al. 2011), and previous Pacific (Griffiths et al. 2005; Whan et al. 2014a) studies. We found a widespread increase of mean temperature, fewer cool extremes and more warm extremes over the past 65 yr, although there were inconsistencies at an index level. For example, the results of this study showed stronger TX90p and TN90p trends (as compared with TX10p and TN10p), which is consistent with the Caribbean (Stephenson et al. 2014) and

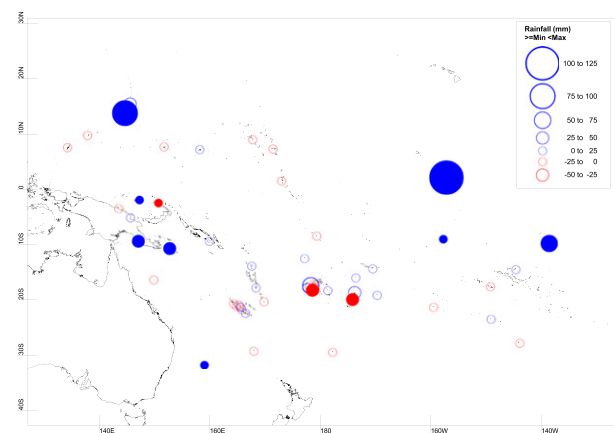


FIG. 9. Observed changes (differences) in the median values of the 20 largest daily precipitation values (K1–K20; bin 1) for 1951–82 and 1983–2015. Solid circles represent differences in the median values that are significant at the 5% level. The size of the circle is proportional to the magnitude of the trend.

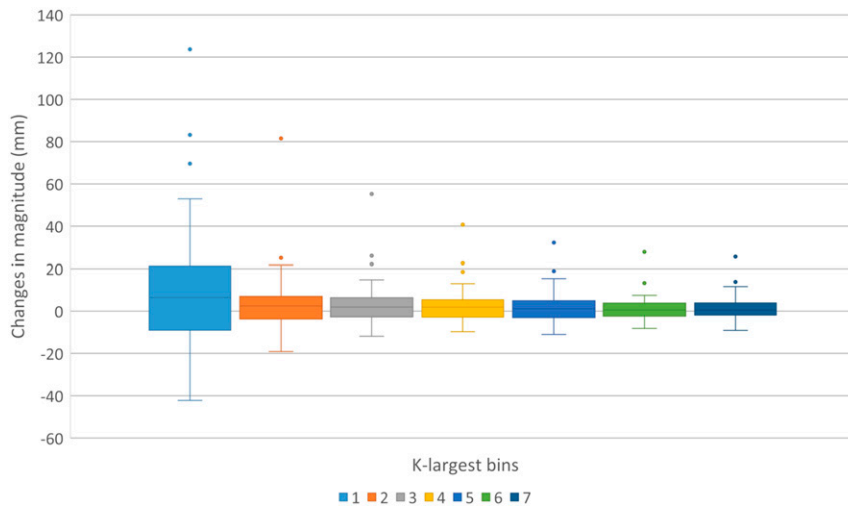


FIG. 10. Observed changes (differences) in the median values for 1983–2015 and 1951–82 for bins 1 (K1–K20) through 7 (K120–K140) for the 52 stations.

Indo-Pacific region (Caesar et al. 2011). However, our results contrast with an earlier Indo-Pacific (Choi et al. 2009) study, where TN10p and TN90p trends were strongest, and a Pacific islands study (Whan et al. 2014a), where there was little difference between the four percentile indices. While differences may be partially due to station selection and an increase in data availability in recent years, Nicholls et al. (2005), found the numbers of warm nights and hot days increased substantially across most of the East Asia–western Pacific region in the year after the onset of El Niño events, while the number of cool days and cold nights tended to decrease. Further, Nicholls et al. (2005) found that the relationship is confounded, at least for warm nights and hot days, by a strong increasing trend in air temperature and the number of extremes, not matched by a trend in the index of the El Niño.

Changes in total and extreme precipitation were more complex. For this study, positive trends were only identified in annual and MAM precipitation at two locations, both in the central Pacific. Annual, MAM, SON, and, to a lesser extent, the DJF total precipitation maps show an El Niño–like pattern in which the ITCZ was displaced south toward the equator and the SPCZ was displaced northeast toward the central Pacific. Previous studies attributed this displacement to ENSO and IPO (Salinger et al. 2001). Increases in mean annual precipitation of 30% or more occurred northeast of the SPCZ between the most recent positive phase of the IPO (1978–98), and the previous negative phase (1946–77). Trends in precipitation in this study with IPO removed show little difference to trends in precipitation with IPO present. This may in part be due to

there being a nonsignificant trend in IPO over 1951–2015.

A statistically significant drying trend in annual total precipitation since the 1950s in the South Pacific subtropics has previously been identified by Jovanovic et al. (2012) and McGree et al. (2014). Jovanovic et al. (2012) noted there was a stronger precipitation decline since 1970. Negative annual total precipitation trends were also found in this study, along with declines in annual CWD and a positive trend in annual CDD. Strong drying trends were identified in the low to moderate extremes indices in JJA and SON in this study. The drying trend was also present in the drought indices that cover the JJA and SON periods.

Declines in annual and DJF total precipitation were found in the southwest French Polynesia region. There was a decrease in moderate- to high-intensity precipitation events, especially those experienced over multiple days in this region. For the multiday absolute indices, the negative trends occurred in DJF, while for R10mm the negative trends occur in SON and for R20mm in MAM. Declines were also present in the annual percentile-based trends (R95p, R95pTOT, R99p, and R99pTOT) and SDII. These negative trends contributed to an increase in meteorological drought (SPI-3 for February and SPI-6 for April) over the extended summer period. On the other hand, there was an increase in the R1mm and decrease in CDD in JJA. These results suggest there have been fewer tropical disturbances in the southwest French Polynesia region in recent decades.

Previous studies associated the drying trend in the western southern subtropics with broader trends seen in parts of southern and eastern Australia. This result is

consistent with a general intensification of the subtropical ridge of high pressure and associated declines in baroclinicity (Timbal 2009; Timbal and Drosowsky 2013; Whan et al. 2014b). Austral summer drying in the southwest French Polynesia subregion, also shown in 1979–2010 twentieth-century reanalysis plots in Fyfe et al. (2012), has been linked with anthropogenic greenhouse gas and ozone changes. A clear poleward shift of the Southern Hemisphere jet stream has also been observed for DJF in reanalyses (Swart and Fyfe 2012). This is attributed largely to a trend in the southern annular mode driven by ozone depletion (Thompson et al. 2011). Drying in the southern French Polynesia region and farther east is also evident in CMIP5 twenty-first-century projections. According to Widlansky et al. (2013) this feature can be related to the anomalous transport of dry subtropical air into the SPCZ region, which is shown to be a result of increased meridional SST gradients in the southeastern tropical Pacific.

On a regional scale, differences in the most extreme daily precipitation (largest 140 values) between 1951–82 and 1983–2015 were not statistically significant. On a station scale there was considerable variability across the region. For the largest 20 values, 11 of 52 stations showed significant change, 8 of which were positive, including 6 within the equatorial region. In response to concerns that the most extreme precipitation has increased in recent decades, we find little evidence of such change at a regional level, but on the subregional level precipitation increased in the equatorial Pacific over parts of PNG and in the central Pacific (eastern Kiribati, the northern Cook Islands, and the northern French Polynesia region). Clearly at the western Pacific scale it is more difficult to show significant changes in climate.

We note with concern the continued decline in data quality and frequency of observations in the western Pacific. Temperature observations >80% complete are now largely limited to the principal observation stations in each country. Notable absences for this study were recent data for Wewak, Momote, and Madang in PNG. These temperature records begin in the 1950s but there are significant gaps in the record in the last decade. Relative to earlier decades, few metadata are being documented, and this will continue to hinder the homogenization of meteorological records in the future. Metadata collection is especially important in the current decade because several Pacific national meteorological services have switched or are in the process of switching to automated observations.

This study will be followed by an investigation into potential relationships between the ET-SCI indices for selected locations and sectoral data for the same location, for

example, sugarcane yield near Nadi Airport, Fiji, stream discharge near Noumea, New Caledonia, and possibly copra yield around Tahiti, French Polynesia.

Acknowledgments. Approval from the respective heads of the Pacific Island national meteorological and hydrological services for the continued use of their meteorological data is greatly appreciated. The authors are particularly grateful to Blair Trewin for his methodological recommendations and Mark Caughey for his analytical assistance. The authors thank the reviewers for their comments and contributions.

REFERENCES

- Aguilar, E., and M. Prohom, 2011: RCLimDex-extraQC (EXTRAQC Quality Control Software) user manual. Centre for Climate Change, University Rovira i Virgili, Tarragona, Spain, accessed 20 March 2016, http://www.c3.urv.cat/data/Manual_rclimdex_extraQC.r.pdf.
- , and Coauthors, 2009: Changes in temperature and precipitation extremes in western central Africa, Guinea Conakry, and Zimbabwe, 1955–2006. *J. Geophys. Res.*, **114**, D02115, <https://doi.org/10.1029/2008JD011010>.
- Alexander, L. V., 2016: Global observed long-term changes in temperature and precipitation extremes: A review of progress and limitations in IPCC assessments and beyond. *Wea. Climate Extremes*, **11**, 4–16, <https://doi.org/10.1016/j.wace.2015.10.007>.
- , and N. Herold, 2015: ClimPACTv2 indices and software. WMO Commission for Climatology Expert Team on Sector-Specific Climate Indices, accessed 19 February 2016, <https://github.com/ARCCSS-extremes/climpact2>.
- , and Coauthors, 2006: Global observed changes in daily climate extremes of temperature and precipitation. *J. Geophys. Res.*, **111**, D05109, <https://doi.org/10.1029/2005JD006290>.
- , P. Uotila, and N. Nicholls, 2009: Influence of sea surface temperature variability on global temperature and precipitation extremes. *J. Geophys. Res.*, **114**, D18116, <https://doi.org/10.1029/2009JD012301>.
- Australian Bureau of Meteorology and CSIRO, 2011a: Regional review. Vol. 1, *Climate Change in the Pacific: Scientific Assessment and New Research*, Pacific Climate Change Science Program, 272 pp., <https://www.pacificclimatechangescience.org/wp-content/uploads/2013/08/Climate-Change-in-the-Pacific-Scientific-Assessment-and-New-Research-Volume-1.-Regional-Overview.pdf>.
- , 2011b: Country reports. Vol. 2, *Climate Change in the Pacific: Scientific Assessment and New Research*, Pacific Climate Change Science Program, 288 pp., <https://www.pacificclimatechangescience.org/wp-content/uploads/2013/09/Volume-2-country-reports.pdf>.
- , 2014: Climate variability, extremes and change in the western tropical Pacific: New science and updated country reports 2014. Pacific-Australia Climate Change Science and Adaptation Planning Program Tech. Rep., 372 pp., https://www.pacificclimatechangescience.org/wp-content/uploads/2014/07/PACCSAP_CountryReports2014_WEB_140710.pdf.
- Caesar, J., and Coauthors, 2011: Changes in temperature and precipitation extremes over the Indo-Pacific region from 1971 to 2005. *Int. J. Climatol.*, **31**, 791–801, <https://doi.org/10.1002/joc.2118>.

- Choi, G., and Coauthors, 2009: Changes in means and extreme events of temperature and precipitation in the Asia-Pacific Network region, 1955–2007. *Int. J. Climatol.*, **29**, 1906–1925, <https://doi.org/10.1002/joc.1979>.
- Field, C. B., V. Barros, T. F. Stocker, and Q. Dahe, Eds., 2012: *Managing the Risks of Extreme Events and Disasters to Advance Climate Change Adaptation*. Cambridge University Press, 582 pp.
- Folland, C. K., J. A. Renwick, M. J. Salinger, and A. B. Mullan, 2002: Relative influences of the interdecadal Pacific oscillation and ENSO on the South Pacific convergence zone. *Geophys. Res. Lett.*, **29**, 21–24, <https://doi.org/10.1029/2001GL014201>.
- , M. J. Salinger, N. Jiang, and N. A. Rayner, 2003: Trends and variations in South Pacific island and ocean surface temperatures. *J. Climate*, **16**, 2859–2874, [https://doi.org/10.1175/1520-0442\(2003\)016<2859:TAVISP>2.0.CO;2](https://doi.org/10.1175/1520-0442(2003)016<2859:TAVISP>2.0.CO;2).
- Fyfe, J. C., N. P. Gillett, and G. J. Marshall, 2012: Human influence on extratropical Southern Hemisphere summer precipitation. *Geophys. Res. Lett.*, **39**, L23711, <https://doi.org/10.1029/2012GL054199>.
- Griffiths, G. M., M. J. Salinger, and I. Leleu, 2003: Trends in extreme daily rainfall across the South Pacific and relationship to the South Pacific convergence zone. *Int. J. Climatol.*, **23**, 847–869, <https://doi.org/10.1002/joc.923>.
- , and Coauthors, 2005: Change in mean temperature as a predictor of extreme temperature change in the Asia–Pacific region. *Int. J. Climatol.*, **25**, 1301–1330, <https://doi.org/10.1002/joc.1194>.
- Guerreiro, S. B., H. J. Fowler, R. Barbero, S. Westra, G. Lenderink, S. Blenkinsop, E. Lewis, and X.-F. Li, 2018: Detection of continental-scale intensification of hourly rainfall extremes. *Nat. Climate Change*, **8**, 803–807, <https://doi.org/10.1038/s41558-018-0245-3>.
- Henley, B., J. Gergis, D. Karoly, S. Power, J. Kennedy, and C. Folland, 2015: A triple index for the interdecadal Pacific oscillation. *Climate Dyn.*, **45**, 3077–3090, <https://doi.org/10.1007/s00382-015-2525-1>.
- IPCC, 2001: *Climate Change 2001: Impacts, Adaptation and Vulnerability*. Cambridge University Press, 1032 pp.
- Jones, D. A., and Coauthors, 2013: An updated analysis of homogeneous temperature data at Pacific Island stations. *Aust. Meteor. Oceanogr. J.*, **63**, 285–302, <https://doi.org/10.22499/2.6302.002>.
- Jovanovic, B., K. Braganza, D. Collins, and D. Jones, 2012: Climate variations and change evident in high-quality climate data for Australia's Antarctic and remote island weather stations. *Aust. Meteor. Oceanogr. J.*, **62**, 247–261, <https://doi.org/10.22499/2.6204.005>.
- Karl, T. R., and R. W. Knight, 1997: The 1995 Chicago heat wave: How likely is a recurrence? *Bull. Amer. Meteor. Soc.*, **78**, 1107–1120, [https://doi.org/10.1175/1520-0477\(1997\)078<1107:TCHWHL>2.0.CO;2](https://doi.org/10.1175/1520-0477(1997)078<1107:TCHWHL>2.0.CO;2).
- Kenyon, J., and G. C. Hegerl, 2008: Influence of modes of climate variability on global temperature extremes. *J. Climate*, **21**, 3872–3889, <https://doi.org/10.1175/2008JCLI2125.1>.
- Lough, J. M., G. A. Meehl, and M. J. Salinger, 2011: Observed and projected changes in surface climate of the tropical Pacific. *Vulnerability of the Tropical Pacific Fisheries and Aquaculture to Climate Change*, J. D. Bell, J. E. Johnson, and A. J. Hobday, Eds., Secretariat of the Pacific Community, 49–99.
- Mann, H. B., and D. R. Whitney, 1947: On a test of whether one of two random variables is stochastically larger than the other. *Ann. Math. Stat.*, **18**, 50–60, <https://doi.org/10.1214/aoms/1177730491>.
- Manton, M. J., and Coauthors, 2001: Trends in extreme daily rainfall and temperature in Southeast Asia and the South Pacific: 1961–1998. *Int. J. Climatol.*, **21**, 269–284, <https://doi.org/10.1002/joc.610>.
- McGree, S., and Coauthors, 2014: An updated assessment of trends and variability in total and extreme rainfall in the western Pacific. *Int. J. Climatol.*, **34**, 2775–2791, <https://doi.org/10.1002/joc.3874>.
- , S. Schreider, and Y. Kuleshov, 2016: Trends and variability in droughts in the Pacific islands and northeast Australia. *J. Climate*, **29**, 8377–8397, <https://doi.org/10.1175/JCLI-D-16-0332.1>.
- McKee, T. B., N. J. Doeskin, and J. Kleist, 1993: The relationship of drought frequency and duration to time scales. *Eighth Conf. on Applied Climatology*, Anaheim, CA, Amer. Meteor. Soc., 179–184.
- Nairn, J. R., and R. J. B. Fawcett, 2015: The excess heat factor: A metric for heatwave intensity and its use in classifying heatwave severity. *Int. J. Environ. Res. Public Health*, **12**, 227–253, <https://doi.org/10.3390/ijerph120100227>.
- Nicholls, N., and Coauthors, 2005: The El Niño–Southern Oscillation and daily temperature extremes in East Asia and the west Pacific. *Geophys. Res. Lett.*, **32**, L16714, <https://doi.org/10.1029/2005GL022621>.
- Page, C. M., and Coauthors, 2004: Data rescue in the Southeast Asia and South Pacific region: Challenges and opportunities. *Bull. Amer. Meteor. Soc.*, **85**, 1483–1489, <https://doi.org/10.1175/BAMS-85-10-1483>.
- Perkins, S. E., 2015: A review on the scientific understanding of heatwaves—Their measurement, driving mechanisms, and changes at the global scale. *Atmos. Res.*, **164–165**, 242–267, <https://doi.org/10.1016/j.atmosres.2015.05.014>.
- , and L. V. Alexander, 2013: On the measurement of heat waves. *J. Climate*, **26**, 4500–4517, <https://doi.org/10.1175/JCLI-D-12-00383.1>.
- Peterson, T. C., and M. J. Manton, 2008: Monitoring changes in climate extremes: A tale of international collaboration. *Bull. Amer. Meteor. Soc.*, **89**, 1266–1271, <https://doi.org/10.1175/2008BAMS2501.1>.
- Rayner, N. A., D. E. Parker, E. B. Horton, C. K. Folland, L. V. Alexander, D. P. Rowell, E. C. Kent, and A. Kaplan, 2003: Global analyses of sea surface temperature, sea ice, and night marine air temperature since the late nineteenth century. *J. Geophys. Res.*, **108**, 4407, <https://doi.org/10.1029/2002JD002670>.
- Salinger, M. J., R. E. Basher, B. B. Fitzharris, J. E. Hay, P. D. Jones, J. P. Macveigh, and I. Schmidely-Leleu, 1995: Climate trends in the south-west Pacific. *Int. J. Climatol.*, **15**, 285–302, <https://doi.org/10.1002/joc.3370150305>.
- , J. A. Renwick, and A. B. Mullan, 2001: Interdecadal Pacific oscillation and South Pacific climate. *Int. J. Climatol.*, **21**, 1705–1721, <https://doi.org/10.1002/joc.691>.
- , S. McGree, F. Beucher, S. B. Power, and F. Delage, 2014: A new index for variations in the position of the South Pacific convergence zone 1910/11–2011/2012. *Climate Dyn.*, **43**, 881–892, <https://doi.org/10.1007/s00382-013-2035-y>.
- Sen, P. K., 1968: Estimates of the regression coefficient based on Kendall's tau. *J. Amer. Stat. Assoc.*, **63**, 1379–1389, <https://doi.org/10.1080/01621459.1968.10480934>.
- Stephenson, T. S., and Coauthors, 2014: Changes in extreme temperature and precipitation in the Caribbean region, 1961–2010. *Int. J. Climatol.*, **34**, 2957–2971, <https://doi.org/10.1002/joc.3889>.

- Svoboda, M., M. Hayes, and D. Wood, 2012: Standardized precipitation index user guide. WMO No. 1090, 24 pp., http://www.wamis.org/agm/pubs/SPI/WMO_1090_EN.pdf.
- Swart, N. C., and J. C. Fyfe, 2012: Observed and simulated changes in the Southern Hemisphere surface westerly wind-stress. *Geophys. Res. Lett.*, **39**, L16711, <https://doi.org/10.1029/2012GL052810>.
- Thompson, D. W. J., S. Solomon, P. J. Kushner, M. H. England, K. M. Grise, and D. J. Karoly, 2011: Signatures of the Antarctic ozone hole in Southern Hemisphere surface climate change. *Nat. Geosci.*, **4**, 741–749, <https://doi.org/10.1038/ngeo1296>.
- Timbal, B., 2009: The continuing decline in South-East Australian rainfall—Update to May 2009. *CAWCR Res. Lett.*, **2**, 4–12.
- , and W. Drosowsky, 2013: The relationship between the decline of southeastern Australian rainfall and the strengthening of the subtropical ridge. *Int. J. Climatol.*, **33**, 1021–1034, <https://doi.org/10.1002/joc.3492>.
- Trewin, B., 2010: Exposure, instrumentation, and observing practice effects on land temperature measurements. *Wiley Interdiscip. Rev.: Climate Change*, **1**, 490–506, <https://doi.org/10.1002/wcc.46>.
- , 2013: A daily homogenized temperature data set for Australia. *Int. J. Climatol.*, **33**, 1510–1529, <https://doi.org/10.1002/joc.3530>.
- Vicente-Serrano, S. M., S. Beguería, and J. I. López-Moreno, 2010: A multiscalar drought index sensitive to global warming: The standardized precipitation evapotranspiration index. *J. Climate*, **23**, 1696–1718, <https://doi.org/10.1175/2009JCLI2909.1>.
- Vincent, L. A., X. L. Wang, E. J. Milewska, H. Wan, F. Yang, and V. Swail, 2012: A second generation of homogenized Canadian monthly surface air temperature for climate trend analysis. *J. Geophys. Res.*, **117**, D18110, <https://doi.org/10.1029/2012JD017859>.
- Wang, X. L., 2008a: Accounting for autocorrelation in detecting mean shifts in climate data series using the penalized maximal t or F test. *J. Appl. Meteor. Climatol.*, **47**, 2423–2444, <https://doi.org/10.1175/2008JAMC1741.1>.
- , 2008b: Penalized maximal F test for detecting undocumented mean shift without trend change. *J. Atmos. Oceanic Technol.*, **25**, 368–384, <https://doi.org/10.1175/2007JTECHA982.1>.
- , and Y. Feng, 2013: RHtestsV4 user manual. CLIVAR and WMO, 28 pp., http://etccdi.pacificclimate.org/RHtest/RHtestsV4_UserManual_10Dec2014.pdf.
- , Q. H. Wen, and Y. Wu, 2007: Penalized maximal t test for detecting undocumented mean change in climate data series. *J. Appl. Meteor. Climatol.*, **46**, 916–931, <https://doi.org/10.1175/JAM2504.1>.
- Whan, K., and Coauthors, 2014a: Trends and variability of temperature extremes in the tropical Western Pacific. *Int. J. Climatol.*, **34**, 2585–2603, <https://doi.org/10.1002/joc.3861>.
- , B. Timbal, and J. Lindesay, 2014b: Linear and nonlinear statistical analysis of the impact of sub-tropical ridge intensity and position on south-east Australian rainfall. *Int. J. Climatol.*, **34**, 326–342, <https://doi.org/10.1002/joc.3689>.
- Widlansky, M. J., A. Timmermann, K. Stein, S. McGregor, N. Schneider, M. H. England, M. Lengaigne, and W. Cai, 2013: Changes in South Pacific rainfall bands in a warming climate. *Nat. Climate Change*, **3**, 417, <https://doi.org/10.1038/nclimate1726>.
- Zhang, X., and F. Yang, 2004: RClimDex (1.0) user manual. CLIVAR and WMO, accessed 20 February 2016, <http://etccdi.pacificclimate.org/RClimDex/RClimDexUserManual.doc>.
- , L. A. Vincent, W. D. Hogg, and A. Niitsoo, 2000: Temperature and precipitation trends in Canada during the 20th century. *Atmos.–Ocean*, **38**, 395–429, <https://doi.org/10.1080/07055900.2000.9649654>.
- , and Coauthors, 2005: Trends in Middle East climate extreme indices from 1950 to 2003. *J. Geophys. Res.*, **110**, D22104, <https://doi.org/10.1029/2005JD006181>.
- , L. Alexander, G. C. Hegerl, P. Jones, A. Klein Tank, T. C. Peterson, B. Trewin, and F. W. Zwiers, 2011: Indices for monitoring changes in extremes based on daily temperature and precipitation data. *Wiley Interdiscip. Rev.: Climate Change*, **2**, 851–870, <https://doi.org/10.1002/wcc.147>.
- Zhou, Y., and G. Ren, 2011: Change in extreme temperature event frequency over mainland China, 1961–2008. *Climate Res.*, **50**, 125–139, <https://doi.org/10.3354/cr01053>.

Copyright of Journal of Climate is the property of American Meteorological Society and its content may not be copied or emailed to multiple sites or posted to a listserv without the copyright holder's express written permission. However, users may print, download, or email articles for individual use.